Resource

Immunity

Antigen-level resolution of commensal-specific B cell responses can be enabled by phage display screening coupled with B cell tetramers

Graphical abstract

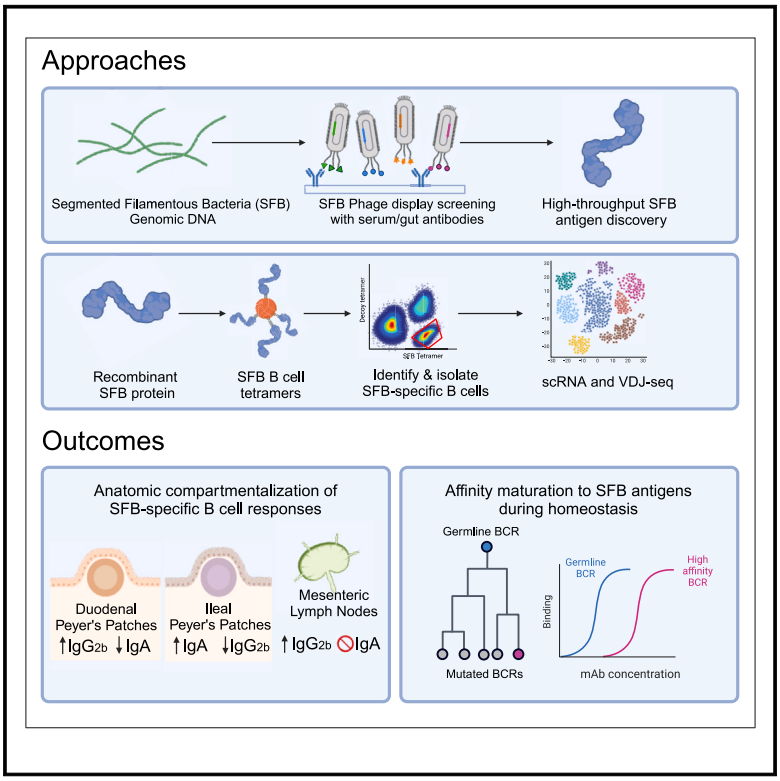

Highlights

- Phage display screening identifies immunogenic commensal antigens
- B cell antigen tetramers enable identification of SFB-specific B cells
- SFB-specific B cells display anatomically compartmentalized effector functions
- Affinity maturation of SFB-specific B cells occurs under homeostatic conditions

Authors

Sheenam Verma, Matthew J. Dufort, Tayla M. Olsen, ..., Sam Scharffenberger, Andrew T. McGuire, Oliver J. Harrison

Correspondence

oharrison@benaroyaresearch.org

In brief

Adaptive immunity to commensal microbes promotes tissue homeostasis, immunity, and repair, but approaches to identify commensal-specific B cell responses are lacking. Verma et al. utilize phage display screening and subsequent generation of B cell tetramers to identify anatomical compartmentalization of SFB-specific B cell responses in gut-associated lymphoid tissues.

Verma et al., 2024, Immunity 57, 1428–1441
June 11, 2024
https://doi.org/10.1016/j.immuni.2024.04.014

CellPress

CellPress

Immunity

Resource

Antigen-level resolution of commensal-specific B cell responses can be enabled by phage display screening coupled with B cell tetramers

Sheenam Verma,[1] Matthew J. Dufort,[2] Tayla M. Olsen,[1,3] Samantha Kimmel,[1] Jasmine C. Labuda,[1] Sam Scharffenberger,[4,6] Andrew T. McGuire,[4,5,6] and Oliver J. Harrison[1,3,7,8,*]

[1]Center for Fundamental Immunology, Benaroya Research Institute, Seattle, WA, USA
[2]Center for Systems Immunology, Benaroya Research Institute, Seattle, WA, USA
[3]Molecular and Cellular Biology Program, University of Washington, Seattle, WA, USA
[4]Vaccine and Infectious Disease Division, Fred Hutchinson Cancer Center, Seattle, WA, USA
[5]Department of Global Health, University of Washington, Seattle, WA, USA
[6]Department of Laboratory Medicine and Pathology, University of Washington, Seattle, WA, USA
[7]Department of Immunology, University of Washington, Seattle, WA, USA
[8]Lead contact
*Correspondence: oharrison@benaroyaresearch.org
https://doi.org/10.1016/j.immuni.2024.04.014

SUMMARY

Induction of commensal-specific immunity contributes to tissue homeostasis, yet the mechanisms underlying induction of commensal-specific B cells remain poorly understood in part due to a lack of tools to identify these cells. Using phage display, we identified segmented filamentous bacteria (SFB) antigens targeted by serum and intestinal antibodies and generated B cell tetramers to track SFB-specific B cells in gut-associated lymphoid tissues. We revealed a compartmentalized response in SFB-specific B cell activation, with a gradient of immunoglobulin A (IgA), IgG1, and IgG2b isotype production along Peyer's patches contrasted by selective production of IgG2b within mesenteric lymph nodes. V(D)J sequencing and monoclonal antibody generation identified somatic hypermutation driven affinity maturation to SFB antigens under homeostatic conditions. Combining phage display and B cell tetramers will enable investigation of the ontogeny and function of commensal-specific B cell responses in tissue immunity, inflammation, and repair.

INTRODUCTION

Immunoglobulin A (IgA) plays a key role in immunity to pathogens, shapes early life interactions with the microbiota, and maintains microbiota diversity and compartmentalization throughout life.[1–4] In the gut, both T cell-independent (TI) and T cell-dependent (TD) mechanisms promote IgA production. TI IgA is considered to primarily recognize conserved microbial structures with relatively low affinity.[5] By contrast, TD IgA is strongly induced by mucus-resident and epithelial-adherent microbes and potently regulates mutualistic relationships with the microbiota.[1,2] TD-IgA induction occurs primarily in the Peyer's patches (PPs) of the small intestine, where activated B cells receive T cell help, perform class-switch recombination (CSR), enter germinal centers (GCs), and undergo somatic hypermutation (SHM) of Ig genes.[6] Commensal-specific IgG antibodies are also generated and can contribute to both host protection during systemic infection[7] and immune regulation at mucosal sites by dampening responses to commensals.[8] How IgG responses to commensal microbes are mounted is poorly understood, in part because it is only recently appreciated that these responses can contribute to synergistic host-microbe interactions during homeostasis.[8–10] While homeostatic IgG production within the intestine is hypothesized to limit bacterial translocation and associated bacteremia, most of our understanding of commensal-specific IgG implicate these responses in disease pathogenesis as elevated concentrations of commensal-specific IgG antibodies, and increased frequencies of colonic IgG$^+$ plasma cells, are routinely observed in patients with inflammatory bowel disease (IBD).[11,12] A better understanding of how commensal-specific IgA and IgG responses are mounted and regulated is therefore important for studies of intestinal homeostasis, immunity, and inflammation.

Mucus-resident and epithelial-adherent microorganisms play a dominant role in directing mucosal immune responses during homeostasis. In humans, non-human primates and rodents, epithelium-associated microorganisms influence the local and systemic activation of the immune system and are implicated in both protection from pathogen infection as well as exacerbation of tissue inflammation and autoimmunity. These species, including *Clostridiales* spp., *Candida* spp., *Akkermansia muciniphila*, and *Helicobacter* spp., all interact closely with the intestinal epithelium,[13–18] a process thought to account for their

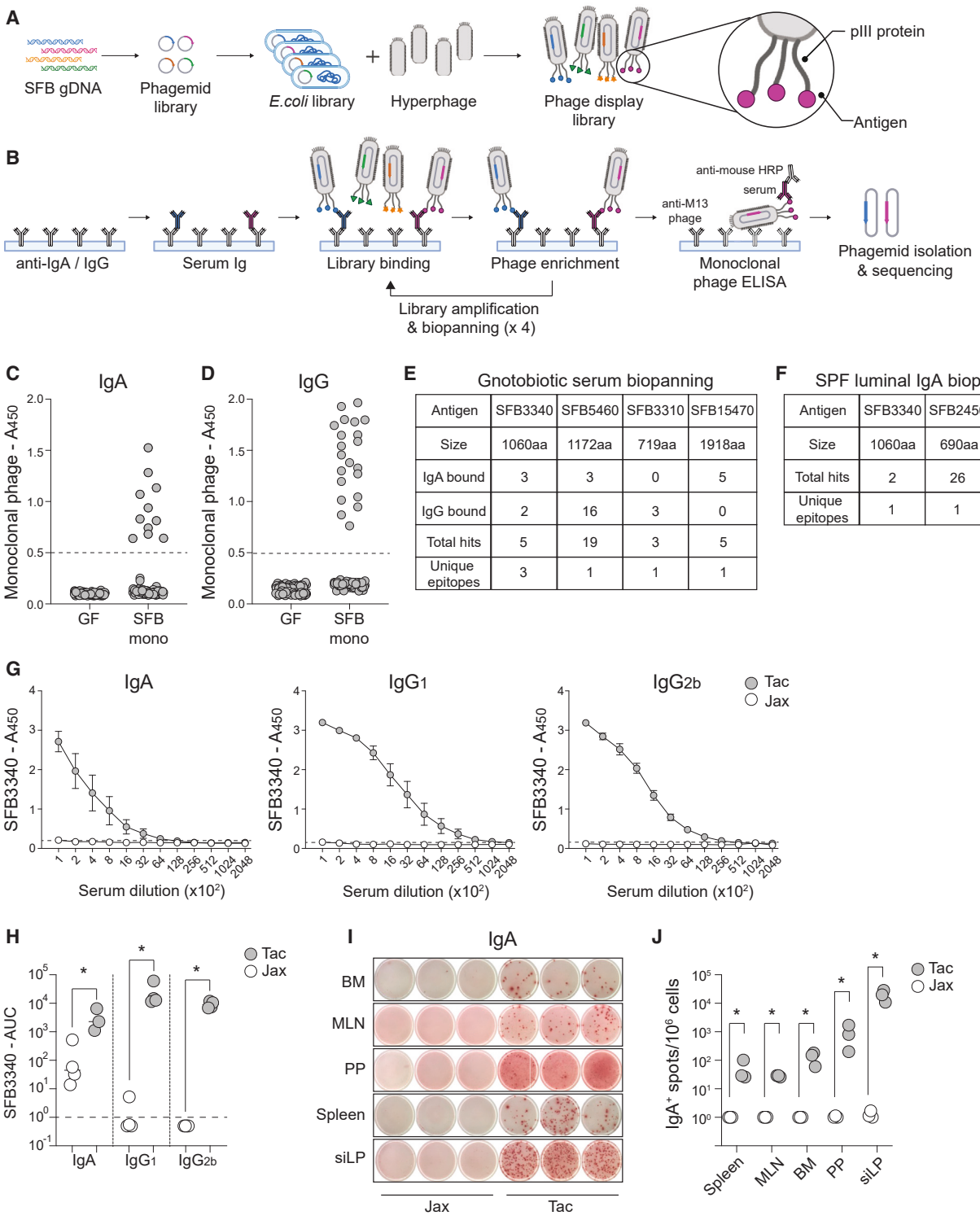

Antigen	SFB3340	SFB5460	SFB3310	SFB15470
Size	1060aa	1172aa	719aa	1918aa
IgA bound	3	3	0	5
IgG bound	2	16	3	0
Total hits	5	19	3	5
Unique epitopes	3	1	1	1

Antigen	SFB3340	SFB2450	SFB15470
Size	1060aa	690aa	1918aa
Total hits	2	26	7
Unique epitopes	1	1	1

Figure 1. Phage display screening identifies immunogenic B cell antigens in segmented filamentous bacteria

(A) Schematic of generation of SFB antigen phage display library.

(B) Schematic of phage display biopanning using SFB antigen library and antibodies from germ-free and SFB-monocolonized gnotobiotic mice.

(C and D) Identification of immunogenic antigen hits using serum from germ-free or SFB monocolonized mice, assessed by binding of enriched monoclonal phage to immobilized IgA (C), or IgG (D).

(E) Features of the 4 immunogenic SFB proteins identified by phage display using serum antibodies from SFB monocolonized mice.

(F) Features of the 3 immunogenic SFB proteins identified by phage display using luminal IgA from Taconic B6 WT mice.

(legend continued on next page)

ability to heighten tissue immunity.[19] Thus, investigating how commensal microbes that intimately engage with the intestinal epithelium influence host immunity is key to understanding not only tissue homeostasis but also inflammation. In murine systems, a key example of these species is segmented filamentous bacteria (SFB), which represents a prototypic commensal colonizing the gastrointestinal tract. Indeed, SFB colonization promotes accumulation of T helper 17 (Th17) and Th1 cells in the small intestinal lamina propria (siLP), Th17 and T follicular helper (Tfh) cells in the PPs and production of TD IgA.[20–25] SFB-specific Th17 cell responses have been associated with protection from gastrointestinal infection,[20] as well as disease exacerbation in the contexts of autoimmunity and autoinflammation.[26–28]

Current approaches for interrogating B cell responses to the microbiota rely on immunoprecipitation of IgA- or IgG-coated microbes, followed by 16S rRNA sequencing (IgA sequencing [IgA-seq]/IgG-seq).[13,25,29,30] Such approaches enable species level resolution of immunogenicity but convey little information regarding the anatomic locale or cellular phenotype of B cells responding to individual microbes, nor the microbial antigens targeted. Conversely, elegant efforts to sequence B cell receptors (BCRs) from gut B cells and plasma cells reveal a snapshot of cellular phenotype, but the immunogenic targets of these antibodies require further downstream identification using culture collections or antigen arrays.[31–34] This is a formidable task given the complexity of the microbiota, with thousands of bacterial species each encoding hundreds to thousands of unique proteins, representing an overwhelming number of potential target antigens. We set out to develop a high-throughput means to identify immunogenic antigens from commensal microbes and subsequently conduct studies of commensal-specific IgA and IgG producing B cells at cellular resolution, which to date have not been feasible.

Phage display technology is a high-throughput screening technique used to identify ligands and binding partners for proteins and other macromolecules. This approach also enables identification of antibody binding to thousands of potential antigens in parallel, with previous successful employment identifying immunogenic antigens derived from pathogenic microbes.[35,36] B cell tetramers are increasingly employed as an experimental approach to identify antigen-specific B cells in response to exposure to model antigens, vaccination, and infectious pathogens. Indeed, use of immunogenic proteins from *Plasmodium* spp. and influenza A virus as B cell tetramers has been a key step in identifying aspects of host immunity to these pathogens within systemic and barrier tissues.[37,38] Broader application of these tools to immunogenic commensal microbes would enable breakthroughs in our understanding of the dynamic interactions between the immune system and the microbiota.

In this report, we now combine phage display screening and B cell tetramers to identify immunogenic antigens and profile the ontogeny of B cells specific to commensal antigens *in vivo*. We generated a phage display library derived from genomic DNA of SFB to screen for immunogenic B cell antigens and discovered multiple SFB-derived antigens bound by distinct antibody isotypes. We subsequently generated B cell tetramers to directly identify SFB-specific B cells in the gut-associated lymphoid tissue (GALT) during vertical transmission and *de novo* colonization with SFB, revealing distinct B cell activation states in different anatomical sites. By performing BCR repertoire sequencing and clonal analyses, in conjunction with generating clonal lineages of SFB-specific antibodies, we directly demonstrated a trajectory of affinity maturation to a selected commensal antigen. This approach now enables the phenotypic interrogation of commensal-specific B cells across tissues and time, facilitating future studies of mucosal B cell biology in health and disease.

RESULTS

Phage display library screening identifies immunogenic commensal antigens

We sought to develop a system with which to track antigen-specific B cell responses to commensal microbes within the GALT. To do so, we selected SFB as an immunostimulatory epithelium-adherent microbe capable of modulating host immunity, including induction of TD IgA production.[21] To identify immunogenic protein antigens recognized by SFB-specific B cells, we generated an SFB phage display library and antibody-based biopanning screen, an approach previously used to identify immunogenic B cell antigens in pathogenic microbes.[35,36] To this end, we cloned 200–600 bp fragments of SFB genomic DNA (gDNA) into a phagemid library vector that fuses potential antigens to the M13 phage outer surface protein pIII[39] (Figure 1A). The phagemid library was packaged to form infectious phage using pIII-deficient hyperphage (M13K07ΔgIII), selecting for in-frame pIII-fusion open reading frames (ORFs) by genetic complementation, and generating a phage library consisting of $\sim 5 \times 10^7$ putative SFB antigens (Figure 1A).[39,40] Immobilized serum IgA and IgG antibodies were used to immunoprecipitate SFB epitope-bearing phage (Figure 1B). Specifically, serum from both germ-free and SFB-monocolonized mice was depleted of phage-reactive antibodies and subsequently used to immunoprecipitate SFB antigen-bearing phage. Immunoprecipitated phage were released by trypsin digestion, and amplified by infection of F′ *E. coli*. To identify high-affinity binders, we conducted 4 increasingly stringent biopanning cycles. After enrichment, we isolated 96 individual monoclonal phage and using ELISA, retested individual phage for binding using serum from SFB-monocolonized mice. This resulted in identification

(G) SFB3340-specific ELISA of serum antibody reactivity by WT mice from Jackson Laboratories (Jax) or Taconic Biosciences (Tac). Dashed line represents limit of detection.
(H) SFB3340-specific ELISA binding represented as area under curve (AUC). Dashed line represents limit of detection.
(I and J) Representative images and quantification of SFB3340-specific ELISpot IgA responses from leukocytes isolated from indicated tissues and stimulated with recombinant SFB3340. For phage display (A–F), data represent a single screen conducted with serum pooled from germ-free ($n = 3$) or SFB-monocolonized ($n = 5$) mice or luminal IgA from Taconic B6 WT mice ($n = 3$). For ELISA and ELISpot data (G–J), data shown represent one of at least three independent experiments each with three mice per group. * $p < 0.05$ calculated using Student's t test. ELISA data are represented as mean ± SD.
See also Figure S1.

of 32 monoclonal phage (optical density [O.D.] > 0.5), with all identified phage encoding epitopes derived from the SFB genome (Figures 1C–1E). Stochastic sampling of unbound phage identified both non-immunogenic inserts aligning to the SFB genome but also inserts derived from the mouse genome, representing host gDNA content in fecal samples utilized for phagemid library preparation (data not shown). Among the 32 monoclonal phage, we assigned antigens to 4 SFB-derived proteins (Figures 1E and S1A). Of the four identified antigens, SFB5460, SFB3310, and SFB15470 all had multiple repeat detections of a single immunogenic domain, whereas SFB3340 was identified to be targeted in 3 distinct N-terminal epitopes (Figure S1A). Additionally, while SFB5460 and SFB3340 were targeted by both IgA and IgG, SFB3310 and SFB15470 were bound selectively by IgG or IgA, respectively (Figure 1E). As such, under the conditions of SFB monocolonization, serum antibodies enable identification of immunogenic antigens from a phage display library. To determine whether luminal IgA could also be used for phage display screening, and whether this could be achieved in the context of a complex bacterial community, we screened the same SFB antigen phage library using small intestinal luminal IgA isolated from specific-pathogen-free (SPF) wild-type (WT) C57BL/6 mice from Taconic Biosciences (Tac) that are naturally colonized with SFB. We identified SFB3340 and SFB15470 antigens, also identified using serum IgA, as well as an additional SFB-derived protein SFB2450 (Figures 1F and S1B), demonstrating that both systemic and local antibodies can enable identification of immunogenic antigens by phage display. Thus, phage display screening represents a powerful experimental system with which to identify immunogenic commensal antigens, increasing the granularity of the targets of humoral immunity from the species level afforded by IgA- or IgG-seq to that of individual immunogenic proteins. Notably, and validating our approach, among the immunogenic SFB antigens identified by phage display screening, SFB3340 has also been identified as a target of Th17 and Tfh cell responses elicited by SFB in the siLP and PPs, respectively.[28] Given the previous generation and widespread employment of SFB3340-specific peptide:I-A^b tetramers and T cell receptor transgenic mice, we focused on this antigen to investigate commensal-specific B cells within systemic and gut-associated lymphoid tissues.

Phage display-derived antigens identify commensal-specific B cells *ex vivo*

To validate SFB3340 as a target of mucosal B cells and investigate the extent of targeting of SFB3340 under homeostatic conditions in SPF mice, we performed antigen-specific ELISA and enzyme-linked immunosorbent spot (ELISpot) assays using serum, luminal antibodies, and tissues from naive WT B6 mice naturally colonized (Taconic Biosciences [Tac]) or not (Jackson Laboratories [Jax]), with SFB. SFB3340-specific serum and luminal IgA was readily detectable in SFB-colonized Tac, but not Jax, B6 mice (Figures 1G and S1C), confirming that SFB3340 is indeed targeted in SPF mice containing a diverse commensal microbiota, and reactivity was not an artifact of gnotobiotic environs. Additionally, SFB3340-specific serum IgG1, and IgG2b, but not IgM, IgG2c, IgG3, or IgE, were detected in SFB-colonized Tac B6 mice (Figures 1G, 1H, and S1D). In line with reports that SFB-specific IgA responses are entirely T dependent,[21,25] SFB3340-specific serum IgA, IgG1, and IgG2b were undetectable in *Tcrbd*$^{-/-}$ mice (Figure S1E). Furthermore, these responses were undetectable in both *Icos*$^{-/-}$ and *Bcl6*$^{\Delta CD4}$ mice, demonstrating a requirement for Tfh cells[41,42] (Figures S1F and S1G). To identify the distribution of SFB3340-specific B cells across tissues, we used antigen-specific ELISpot assays. SFB3340-specific B cell responses producing IgA, IgG1, and IgG2b were identified in the spleen, PPs, mesenteric lymph nodes (MLNs), siLP and bone marrow (BM) of Tac, but not Jax mice (Figures 1I, 1J, S1H, and S1I). Together, SFB3340 is the target of Tfh-dependent IgA, IgG1, and IgG2b producing B cells and serves as a tool to investigate the induction of commensal-specific B cells responding to an endogenous antigen under homeostatic conditions.

B cell tetramers enable identification of commensal-specific B cells *ex vivo*

Identification of immunogenic commensal antigens provides an opportunity to address key questions regarding mucosal immunity that are facilitated by direct identification of commensal-specific B cells. B cell antigen tetramers are powerful tools that enable analysis of cellular phenotype, isotype, kinetics, and polyclonal repertoire of antigen-specific B cells. We extended these utilities to study SFB-specific B cells in the GALT, by adopting techniques used to study protein immunization and pathogen infection.[37,43] To this end, we generated phycoerythrin (PE)-conjugated B cell tetramers containing the majority of the SFB3340 protein, lacking the putative N-terminal transmembrane domain (Figure S2A). In all experiments, isolated leukocytes were initially stained with a decoy reagent, to identify and exclude cells binding structural components of the tetramer[43] (Figure S2A). Cells were subsequently stained with SFB3340 tetramers and fluorescent antibodies for analysis by multiparameter flow cytometry, and after excluding non-B cells and doublets, SFB3340$^+$Decoy$^-$ B cells were identified among B220$^+$ and B220^{lo}CD138$^+$ cells (Figure S2B). In naive Jax B6 mice that are not colonized by SFB, the few SFB3340$^+$ B cells identified within PPs were naive follicular B cells (IgD$^+$CD38$^+$GL-7$^-$FAS$^-$), representing the naive immune repertoire (Figures 2A–2C). By contrast, in the PPs of SFB-colonized Tac B6 mice, we identified SFB3340$^+$ B cells with an activated phenotype. Specifically, we identified 77% ± 6% of SFB3340$^+$ B cells to be IgM$^-$IgD$^-$ class-switched (swIg$^+$), compared with 14% ± 4% of non-cognate B cells in Tac B6 mice (Figure 2C). swIg$^+$ SFB3340$^+$ B cells were not detected in PPs of Jax B6 mice, consistent with a requirement of antigen for B cell activation (Figure 2C). Furthermore, nearly all swIg$^+$ SFB3340$^+$ B cells were FAS$^+$CD38$^-$ GC B cells, with few if any FAS$^-$CD38$^+$ memory B cell (MBC) detectable in steady-state mice (Figures 2D and 2E). By contrast, MBC were detectable among the non-cognate repertoire of swIg$^+$ PP B cells (Figures 2D and 2E). A similarly polarized PP GC B cell response to SFB3340 was also detected in SFB monocolonized, but not germ-free mice, and in Jax B6 mice *de novo* colonized with feces from SFB-monocolonized mice (Figures 2F and 2G). Thus, our data demonstrate that SFB3340 B cell tetramers enable direct identification of SFB-specific B cell activation and that SFB colonization is necessary and sufficient to elicit induction of SFB3340$^+$ GC B cell responses within PPs.

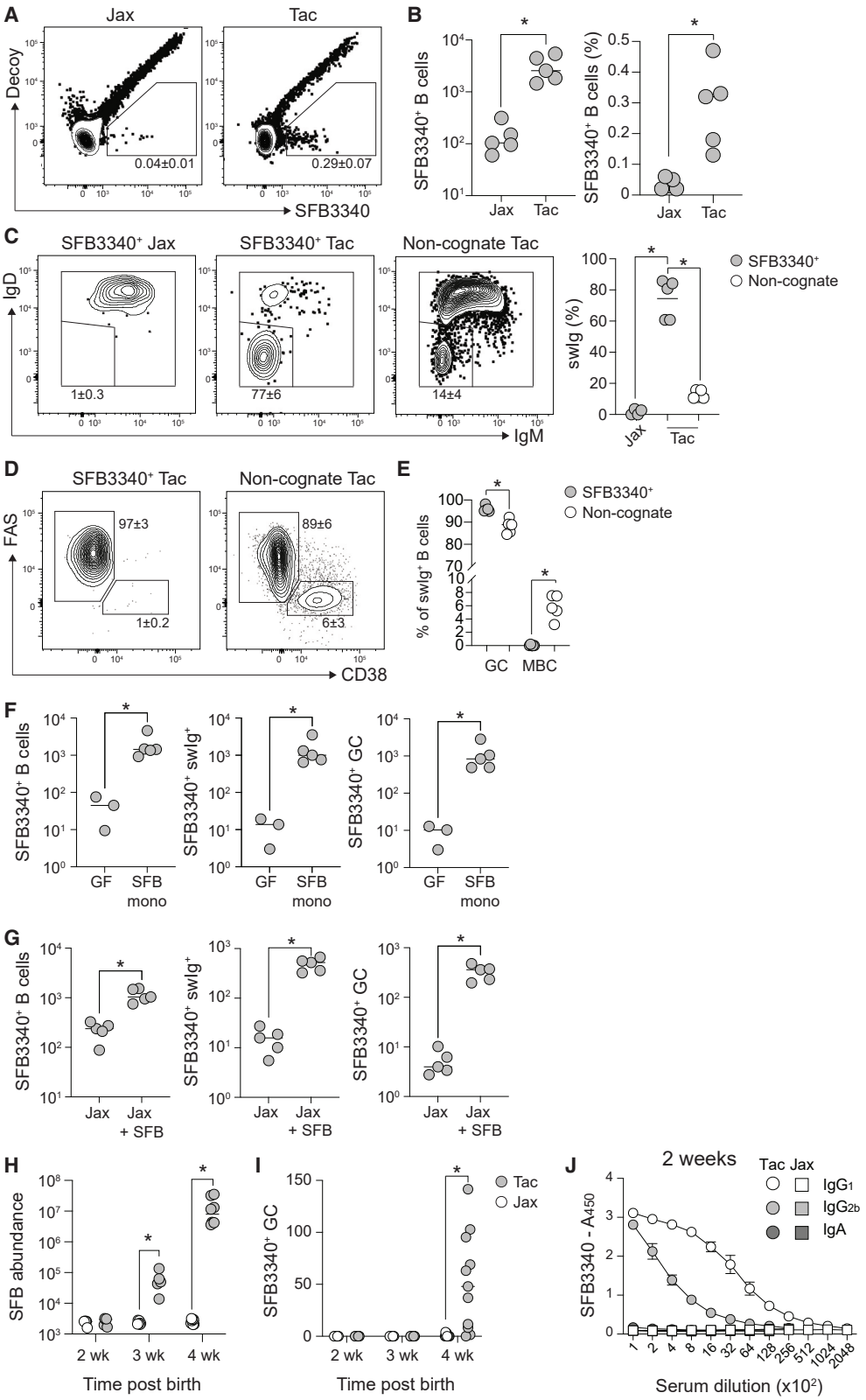

(legend on next page)

A substantial proportion of homeostatic intestinal IgA$^+$ cells in adult mice arise early in life.[44] To investigate the dynamics of early life SFB3340-specific B cell activation during natural colonization by vertical transmission, we conducted parallel timed breeding of Jax B6 and Tac B6 mice. As previously described,[45] SFB colonization was undetectable by qPCR in either strain at 2 weeks of age but readily detectable in Tac B6 mice by 3 weeks of age and reached an abundance observed in adult mice by 4 weeks post-birth (Figure 2H). Induction of SFB3340$^+$ B cell activation in PPs was detectable by 4 weeks of age (Figure 2I). However, and consistent with reports of transplacental transfer of IgG1 and IgG2b,[8] serum antibodies specific to SFB3340 were already detectable in serum by 2 weeks of age, preceding both SFB colonization and SFB3340$^+$ B cell activation (Figure 2J). SFB3340-specific IgA was not detected at this time point, in line with the observation that IgA is not trans-placentally transferred, nor integrated into the circulation following ingestion. As such, SFB3340-specific B cell tetramers enable discrimination of host B cells and maternally derived antibody responses during early life.

Compartmentalized induction of distinct isotypes by SFB3340$^+$ B cells

Recent studies have identified compartmentalized drainage of the intestine by distinct lymph nodes (LNs) within the gut draining lymph node chain.[46–48] Functionally, this process results in specialization of individual gut LNs in priming tolerogenic or pro-inflammatory T cell responses and the subsequent accumulation of regulatory or effector T cell populations in distinct gut segments.[46–48] We investigated whether a similar gradient of specialized differentiation operates for SFB-specific B cells within PPs. Analysis of PPs from duodenal, jejunal, and ileal regions of Tac B6 mice demonstrated clear compartmentalization of antibody isotype production by SFB3340$^+$ B cells. While GC B cell frequency and low IgG$_1$ expression among swIg$^+$ SFB3340$^+$ B cells was stable across PPs from distinct intestinal regions (Figures 3A, 3B, S3A, and S3B), proximal PPs (duodenal and jejunal) were highly enriched in IgG2b$^+$ GC B cells with a lower frequency in ileal PPs (Figures 3B and S3C). By contrast, IgA$^+$ GC B cell frequencies were low in proximal PPs but represented the dominant antibodies produced in ileal PPs (Figures 3B and S3D). To further determine how anatomic locale governs SFB-specific B cell differentiation, we compared total PPs with cells isolated from MLN of adult Tac B6 mice. While swIg$^+$ SFB3340$^+$ B cell responses were detectable in both tissues, the frequency of swIg$^+$ SFB3340$^+$ B cells was lower in MLN (Figure 3C). Though IgA$^+$ GC B cells were readily detected in the polyclonal B cell population, MLN-derived SFB3340$^+$ GC B cells did not produce IgA and instead almost exclusively produced IgG2b antibodies (Figures 3D–3F and S3E–S3H). Therefore, using B cell tetramers, we now demonstrate a clear anatomical compartmentalization of SFB-specific B cell effector functions across the PPs and MLN.

De novo colonization drives SFB3340$^+$ GC B cell induction with a broad range of antibody isotypes

To gain a deeper understanding of the kinetics and phenotype of SFB-specific B cells induced in GALT without the influence of maternal antibodies acquired during vertical transmission,[8] we introduced SFB into adult naive Jax B6 mice by oral gavage. We used filtered fecal contents from SFB-colonized *Rag2*$^{-/-}$*Il2rg*$^{-/-}$ mice, which harbor ~10 fold enriched fecal SFB compared with WT animals, mimicking a previously described strategy using enriched-SFB (eSFB) flora from lymphocyte-deficient *Rag2*$^{-/-}$*Il23r*$^{-/-}$ mice.[49] This approach also benefits from a lack of donor-derived Igs that coat the fecal contents of WT mice, which could influence *de novo* colonization by SFB. We tracked the kinetics and phenotype of SFB3340-specific B cells in GALT in naive mice and mice 7, 14, 21, and 28 days post-colonization (d.p.c.). In concordance with the rate of engraftment and establishment of stable SFB colonization (Figure S4A), activated SFB3340$^+$ B cells were detectable by 14 d.p.c., with the highest engagement of swIg$^+$ SFB3340$^+$ B cells observed at 28 d.p.c. (Figures 4A and 4B). At time points prior to 14 d.p.c., numbers of SFB3340$^+$ B cells were rare, precluding further investigation. By contrast, SFB3340-specific GC B cells were readily detectable from 14 d.p.c. onward (Figures 4C–4E). Kinetic analyses of SFB3340$^+$ B cell isotype expression identified a stable distribution of IgA$^+$, IgG1$^+$ and IgG2b$^+$ cells in the PPs (Figures 4F–4H). Over this time period, IgA and IgG2b$^+$ B cells were maintained at stable relative frequencies, suggesting that IgA$^+$ B cells were not outcompeted in gut GC responses,

Figure 2. Natural SFB colonization promotes SFB3340-specific GC B cell responses in Peyer's patches

(A) Representative contour plots of SFB3340 B cell tetramer and decoy reagent staining by total Peyer's patch B cells isolated from naive WT B6 mice from Jackson Laboratories (Jax) or Taconic Biosciences (Tac).

(B) Total number of SFB3340$^+$ B cells and their frequency among total B cells in Peyer's patches of WT Jax or Tac B6 mice.

(C) Representative contour plots of IgM and IgD expression and frequencies of swIg$^+$ SFB3340$^+$ B cells in Peyer's patches in WT Jax or Tac B6 mice, or non-cognate SFB3340$^-$Decoy$^-$ B cells in Tac B6 WT mice.

(D and E) Representative contour plots and relative frequencies of GC and MBC populations among SFB3340$^+$ or non-cognate B cells in Peyer's patches of SFB-colonized Tac B6 WT mice.

(F) Total numbers of SFB3340$^+$ B cells, SFB3340$^+$ swIg$^+$ B cells, and SFB3340$^+$ GC B cells in germ-free and SFB-monocolonized mice.

(G) Total numbers of SFB3340$^+$ B cells, SFB3340$^+$ swIg$^+$ B cells and SFB3340$^+$ GC B cells in Jax B6 mice colonized, or not, with fecal contents from SFB-monocolonized gnotobiotic mice.

(H–J) Pups from timed Jax or Tac B6 breeders were assessed for SFB colonization, SFB3340-specific serum antibodies and SFB3340-specific B cells at 2, 3, and 4 weeks of age. (H) Quantification of SFB abundance in fecal contents of pups assessed by qPCR, (I) frequencies of SFB3340$^+$ GC in Peyer's patches, and (J) serum antibody titers of SFB3340-specific antibodies in pups of Jax and Tac B6 breeding pairs at indicated time points post birth.

(A–H) Data shown represent one of two independent experiments with three to five mice per group. (I and J) Data shown represent two combined experiments with five to six mice per experimental group. * $p < 0.05$ calculated using Student's t test. ELISA data are represented as mean ± SD.

See also Figure S2.

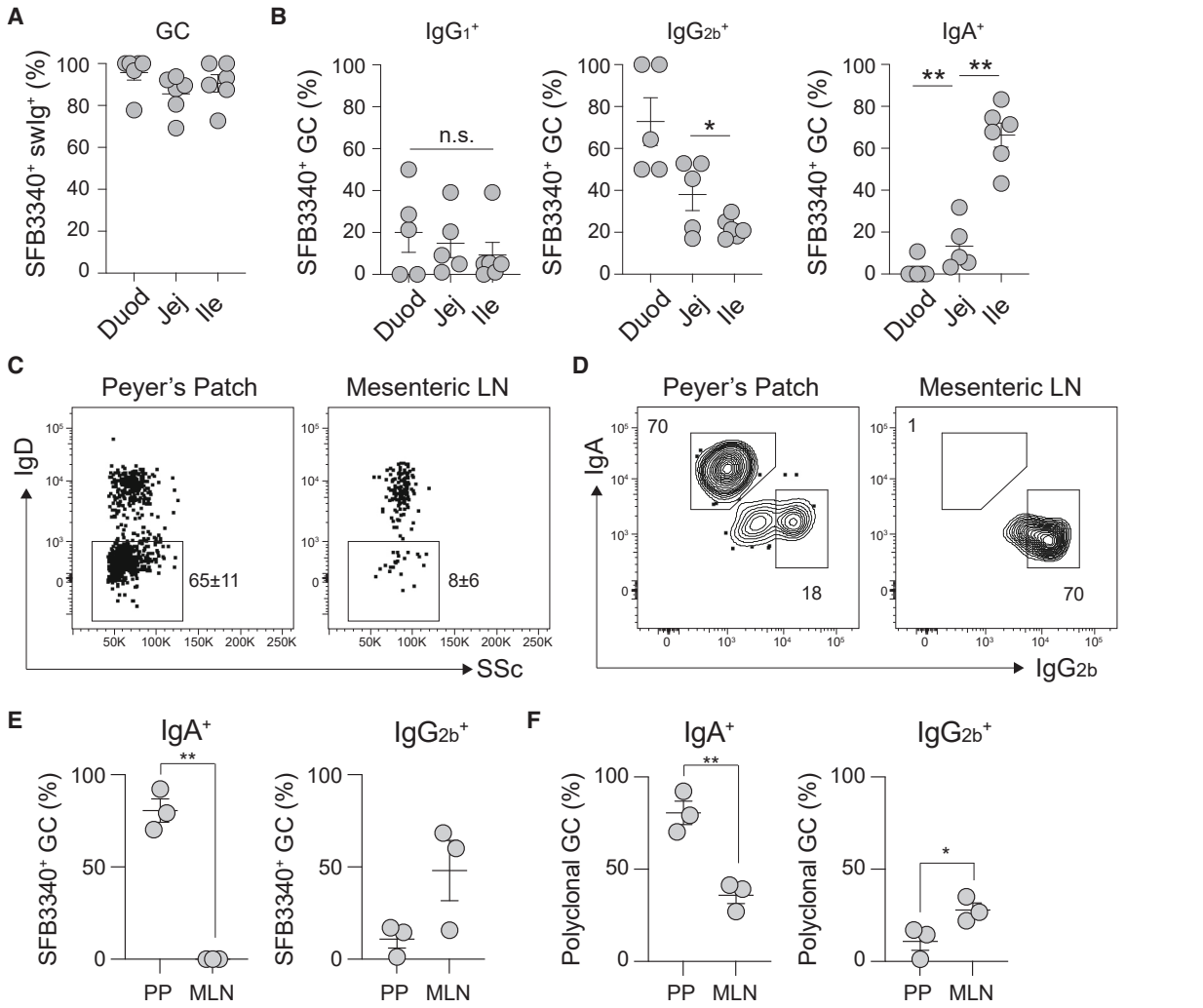

Figure 3. Compartmentalized induction of distinct isotypes to SFB3340 antigen

All mesenteric lymph nodes, or Peyer's patches from distinct intestinal regions of Tac B6 mice were isolated and assayed for SFB3340$^+$ B cell phenotype.

(A and B) (A) Relative frequencies of GC B cells among PP swIg$^+$ SFB3340$^+$ B cells, and (B) relative frequencies of isotype expressing SFB3340$^+$ GC B cells in PP from distinct intestinal sections.

(C) Representative flow cytometry plots and frequencies of swIg$^+$ SFB3340$^+$ B cells in total gut Peyer's patches or mesenteric lymph nodes.

(D and E) (D) Representative flow cytometry plots and (E) frequencies of IgA$^+$ and IgG2b$^+$ SFB3340$^+$ GC B cells in Peyer's patches and MLN.

(F) Relative frequencies of IgA$^+$ and IgG2b$^+$ non-cognate GC B cells in Peyer's patches and MLN.

(A–D) Data shown represents one of two independent experiments with five mice per group. (E and F) Data shown represents one of two independent experiments with three mice per group * $p < 0.05$, ** $p < 0.01$, calculated using Student's t test. Data are represented as mean ± S.D.

See also Figure S3.

in line with recent work demonstrating that heightened IgA BCR-signaling promotes the survival of GC B cells in PPs.[50]

Affinity-driven commensal-specific B cell selection in PP GCs

To date, the antigenic targets of PP B cells undergoing SHM and affinity maturation remain to be determined a priori. However, identification and isolation of single antigen-specific B cells from constitutively active GCs within PPs now enabled us to investigate the selection of gut GC B cells with cellular resolution. As such, we directly investigated the BCR repertoire usage and selection of gut B cells specific to SFB3340 using single-cell RNA sequencing (scRNA-seq) and V(D)J sequencing and identified V(D)J segment usage, clonality, and SHM profiles across SFB3340$^+$ B cells following *de novo* colonization with SFB. To profile the repertoire of multiple mice, total PP cells were isolated from 10 individual WT mice at 21 d.p.c, stained using oligo hash-tagged and fluorescent antibodies, decoy, and SFB3340 tetramer reagents, and subsequently pooled. SFB3340$^+$ B cells from the pooled sample were isolated by fluorescence-activated cell sorting (FACS) and subjected to scRNA-seq and V(D)J sequencing. Deconvolution of oligo hash-tagged antibodies demonstrated that individual mice were evenly represented among high-quality cells, with phenotypic diversity mirroring

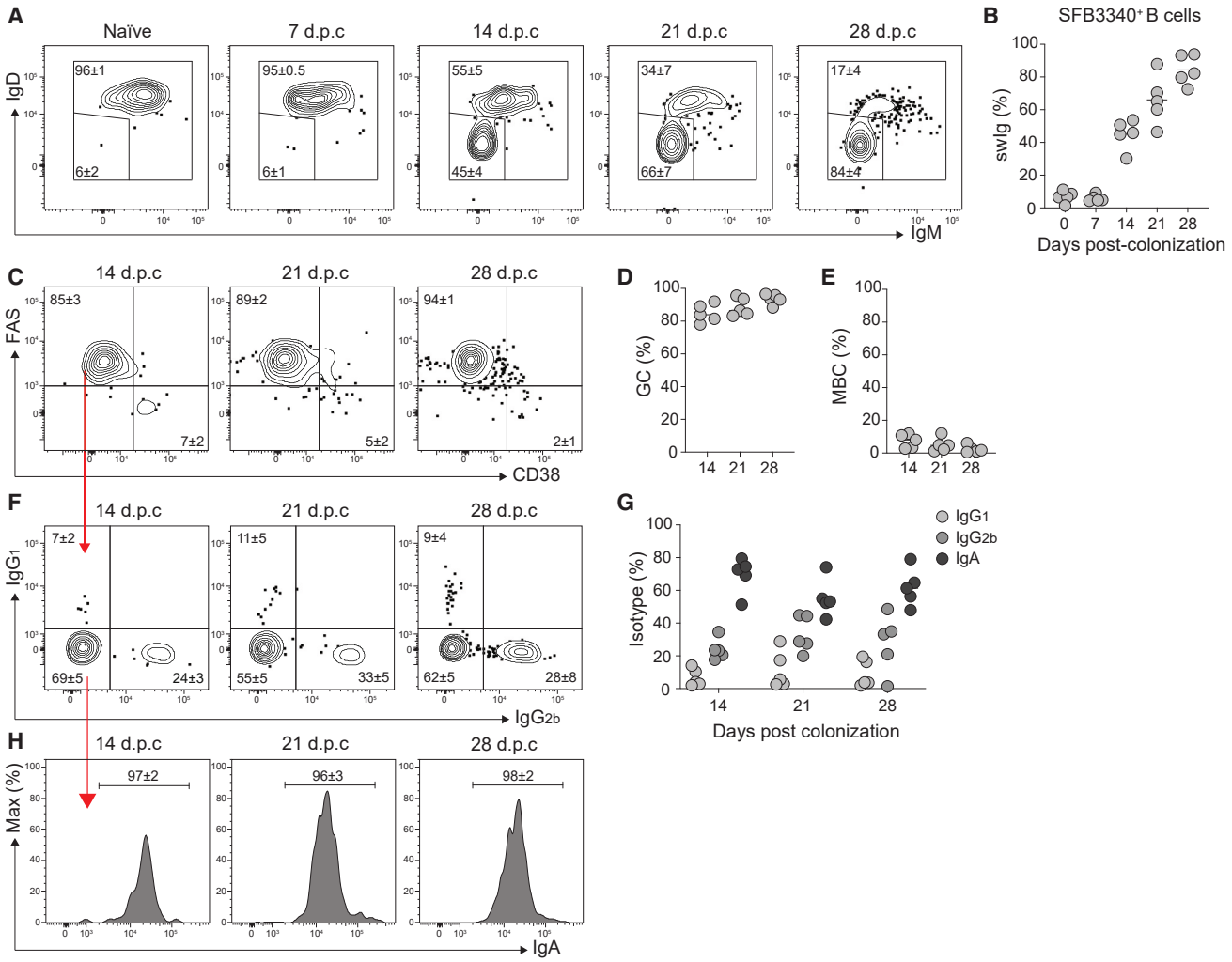

Figure 4. *De novo* colonization with SFB drives SFB3340⁺ GC B cell induction with a broad range of antibody isotypes

Jax B6 WT mice were colonized with SFB by oral gavage of fecal contents from SFB⁺ *Rag2*$^{-/-}$*Il2rg*$^{-/-}$ mice prior to analysis at 7, 14, 21, and 28 days post-colonization (d.p.c). (A) Representative contour plots of IgM and IgD expression by SFB3340⁺ Peyer's patch B cells at indicated time points. (B) Relative frequencies of swIg⁺ SFB3340⁺ B cells in Peyer's patches following SFB colonization. (C) Representative contour plots of GC (FAS⁺CD38⁻) and MBC (CD38⁺FAS⁻) SFB3340⁺ swIg⁺ B cells at 14, 21 and 28 d.p.c. Relative frequencies of SFB3340⁺ GC (D) and MBC (E) at indicated timepoints following SFB colonization. (F) Representative contour plots of IgG1 and IgG2b isotype expression by SFB3340⁺ GC B cells at indicated timepoints following SFB colonization. (G) Quantification of antibody isotype production by SFB3340⁺ GC B cells. (H) Representative contour plots of IgA expression on IgG1⁻IgG2b⁻ SFB3340⁺ GC B cells following SFB colonization. Data shown represents one of three independent experiments each with four to five mice per experimental group.

See also Figure S4.

our cytometric data (Figure S5A). We identified uniform manifold approximation and projection (UMAP) clusters based on marker gene expression, including naive (*Ighd*), GC (*Aicda*) and a small population of antibody-secreting cells (ASCs, [*Prdm1*]) (Figures 5A–5C). Among these cellular populations, antibody isotype identified by scRNA-seq also correlated with cytometric analysis, with a majority of IgA- and IgG2b-producing cells within the GC and ASC populations (Figures 4F–4H and 5B). To investigate BCR repertoire usage by SFB3340⁺ B cells, we mapped the variable heavy chain (V_H) repertoire of productive V(D)J usage across the V_H locus and identified public clonotypes that recurred in GC B cells of multiple mice. We focused on the widespread use of two recurrent clonotypes (RCs), V_H1-76(RC), and V_H1-53(RC), with multiple mice utilizing either, or often both, of these two segments (Figures S5B and S5C). To determine the relationship between clonal selection and affinity maturation of SFB3340⁺ B cells using public V_H1-76(RC) and V_H1-53(RC) clonotypes, we reconstructed BCR evolution for these clonotypes from individual mice and generated phylogenetic trees of inferred SHM acquisition (Figures 5D and 5E). To determine whether acquisition of SHMs contributed to affinity maturation of SFB3340-specific responses, V_H1-53RC-V_k4-58J_k1 and V_H1-76RC-V_k5-43J_k2 antibody families and their unmutated ancestors (UAs) were expressed as monoclonal antibodies (mAb) in a human IgG1 backbone and binding to SFB3340 was assessed. As expected, all recombinant monoclonals from V_H1-53RC-V_k4-58J_k1 and V_H1-76RC-V_k5-43J_k2 families bound SFB3340 protein as assessed by ELISA (Figures 5F and 5G)

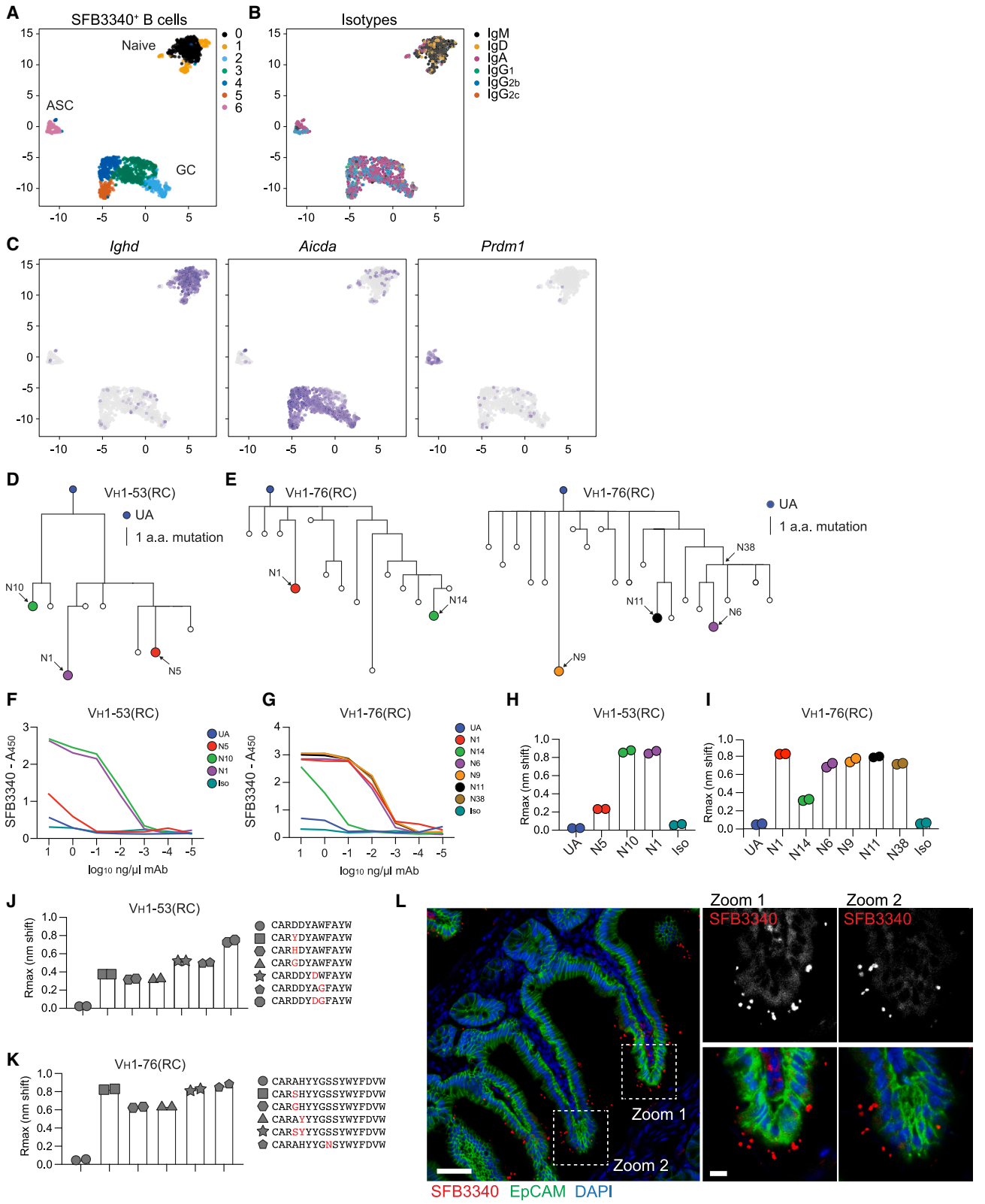

(legend on next page)

and biolayer-interferometry (BLI) (Figures 5H and 5I). Quantification of binding demonstrated a clear increase in binding by both V_H1-53RC-V_k4-58J_k1 (Figures 5F and 5H) and V_H1-76RC-V_k5-43J_k2 (Figures 5G and 5I) antibody lineages bearing somatic mutations. Furthermore, reverting all V_H and variable light chain (V_L) mutations greatly reduced binding of UA antibodies to SFB3340 (Figures 5F–5I), strongly supporting that affinity maturation to SFB3340 occurs in PP GCs. Somatic mutations accumulated within the CDRH3 during BCR evolution (Figure S5D), and experimental introduction of acquired CDRH3 mutations into the UA V_H sequences increased binding even in the presence of UA V_L chains, demonstrating that CDRH3 binding contributed in part to affinity maturation of SFB3340-specific antibody lineages (Figures 5J and 5K). Importantly, recombinant SFB3340-specific antibodies did not bind to irrelevant antigens that are common targets of polyreactive antibodies including Insulin, DNA, lipopolysaccharide (LPS), and ovalbumin[5] (Figure S5E). To demonstrate that recombinant antibodies identified by isolation of SFB3340$^+$ B cells bind SFB3340 antigen in its native conformation, we conducted fluorescence microscopy on ileal tissue sections. Indeed, SFB3340-specific mAb binding identified SFB in close physical proximity to the intestinal epithelium (Figure 5L), confirming that these antibodies recognize SFB *in situ* within ileal tissues. Thus, B cell tetramers enable highly specific isolation of commensal-specific B cells, and SFB3340-specific B cells in PPs undergo SHM and affinity maturation during *de novo* colonization, as demonstrated by increasing binding affinity in antibodies bearing multiple somatic mutations.

DISCUSSION

Host immune responses elicited by commensal microbes influence tissue immunity, inflammation, and repair, but also disease manifestation, severity, and therapeutic efficacy.[9,51] Cognate T cell responses to bacterial components of the gut and skin microbiome play essential roles in maintenance and restoration of tissue integrity during infection and injury. While antibody responses to the microbiota are critical for microbiota containment, diversification, and gut function, our understanding of commensal-specific B cell responses is less developed due to our inability to track cognate responses beyond the community level of gut bacteria, much less the resolution of individual microbes. Although identification of immunogenic commensal microbes using Ig-based enrichment and subsequent 16S rRNA sequencing has shed light on the identity of immunogenic and disease-influencing microbes, identifying the ontogeny and cellular phenotype of B cells producing commensal-specific antibodies remains challenging. Our study details technical innovations that enable mechanistic investigation of antigen-specific B cells within barrier tissues, utilizing high-throughput screening to identify immunogenic commensal antigens, and converting these antigens into experimental reagents with which to identify cognate B cell responses to gut microbes.

Using phage display screening we identified immunogenic antigens derived from SFB, an epithelial-adherent bacterium that resides within the ileum and elicits a TD antibody response detectable in both luminal secretions and serum. The humoral response to *de novo* SFB monocolonization consists of a cognate response and a non-specific component that can be elicited both in PPs and MLNs, but also tertiary lymphoid structures.[52] These aspects of biology are perhaps not unique to SFB, but somewhat distinct from the majority of other commensal microbes. Future studies of other adherent commensal microbes will likely identify a range of mechanisms by which the host generates humoral responses to maintain a state of commensalism. These studies will benefit from the increased resolution of antigenicity afforded by phage display screening. This methodology thus enables use of antigen-specific ELISA or ELISpot to study immunity to a given microbe of interest and allows screening of humoral responses across experimental cohorts. As both luminal and serum antibodies could be used to identify immunogenic antigens by phage display, this approach may also provide utility for studying commensal-specific humoral responses in humans, where intestinal antibody samples may be less readily available than sera, albeit with a caveat that not all commensals elicit serum antibody responses. In this study, phage display screening focused on an intestinal bacterium; however, this approach could also be readily adapted to study non-bacterial components of the microbiota, including fungi, viruses, helminths, protists, as well as our genome-encoded symbionts, endogenous retroviruses. Furthermore, this approach could be employed in studies of immunity in other barrier tissues colonized by commensal microbes including the skin, oral mucosa, and female reproductive tract.

To further investigate the ontogeny, kinetics, phenotype, and anatomic localization of SFB-specific B cells, we generated B

Figure 5. SFB3340$^+$ GC B cells undergo somatic hypermutation and affinity maturation in Peyer's patches under homeostatic conditions

SFB3340$^+$ B cells were isolated by FACS from the Peyer's patches of WT B6 mice *de novo* colonized for 21 days with SFB. Total Peyer's patches from 10 mice were stained with SFB3340 tetramer and oligo hash-tagged antibodies, before pooling, and isolation of SFB3340$^+$ B cells by FACS prior to scRNA-seq using the 10X platform.

(A–C) UMAP plots of (A) scRNA-seq clusters, (B) antibody isotype transcripts, and (C) curated marker genes used to identify naive, GC and antibody-secreting cell clusters.

(D and E) Phylogenetic trees of reconstructed evolution recurrent clonotypes (RCs) of V_H1-76(RC) and V_H1-53(RC) antibody lineages identified from SFB3340$^+$ B cells of individual mice.

(F and G) Mutations are calculated at the amino acid level across the entire VH transcript (F and G) ELISA-based binding of recombinant antibody lineages to recombinant SFB3340.

(H and I) Biolayer inferometry-based binding metrics of recombinant antibody lineages from V_H1-76(RC) and V_H1-53(RC) clonotypes.

(J and K) Biolayer inferometry-based binding metrics of recombinant UA antibodies bearing acquired CDRH3 mutations, to recombinant SFB3340.

(L) Confocal microscopy imaging of V_H1-76(RC) N1 monoclonal antibody (mAb) staining of ileal tissue from an SFB-colonized *Rag2*$^{-/-}$*Ilrg2*$^{-/-}$ mouse. Scale bars in main image: 50 μm, scale bars in inset image: 10 μm. Data were generated from a single scRNA-seq/V(D)J-seq experiment using cells combined from 10 individual mice. ELISA and biolayer-interferometry experiments were conducted three times, and confocal microscopy imaging was conducted twice.

See also Figure S5.

cell tetramers from SFB3340 and established methods to identify SFB-specific cells *ex vivo* at mucosal sites, bridging the current divide between bacteria-level resolution of immunity enabled by IgA- or IgG-seq and the antibody-specificity resulting from sequencing GALT and lamina propria derived BCRs. Notably, this antigen-level resolution revealed compartmentalization of microbiota-specific antibody isotype production along the length of the small intestine, a dichotomy in isotype production between MLNs and PPs, and the kinetics of early life B cell responses to commensal microbes previously obfuscated by inheritance of maternal-derived antibodies. Specifically, we identified a clear anatomical compartmentalization of B cell effector functions with IgA^+ $SFB3340^+$ GC responses enriched in distal PP, and strong enrichment of IgG isotypes within proximal PP and MLN. These discoveries are in line with a model in which microbial components within the MLN might indicate bacterial translocation or infection, wherein the MLN would represent the last component of the mucosal firewall prior to systemic bacterial exposure. In this case, production of IgG isotypes would favor rapid opsonization and clearance of invading microbes. Investigating how the environmental milieu and local T cell populations within distinct PP and MLN influence selection of IgA^+ and IgG^+ B cells in gut GCs is of great interest. In this instance, it is reasonable to hypothesize that compartmentalized B cell effector function across intestinal regions occurs as a direct result of preferential colonization of the ileum by SFB, to which the species has adapted with holdfasts and auxotrophies. Indeed, SFB colonization promotes ileal production of serum amyloid A (SAA), which subsequently licenses interleukin (IL)-17A-production from SFB-specific $ROR\gamma t^+$ $CD4^+$ T cells within the ileal lamina propria, promoting local barrier integrity through antimicrobial peptide production.[49] In an analogous manner, ileal induction of SAA, a carrier of retinol,[53] may promote provision of retinoic acid directly to intestinal B cells to promote IgA responses locally within the intestine.[54] An alternative, but not mutually exclusive possibility, is that because the proximal small intestine is devoid of SFB colonization, it harbors few SFB-specific Th17 cells and thus decreased AMP induction. Within this distinct environment, transient exposure to SFB antigens within the proximal intestine, that likely occur during coprophagia, could preferentially elicit induction of IgG isotypes to prevent bacterial translocation. Ongoing efforts within the laboratory seek to determine how local niche factors influence induction of distinct antibody isotypes by SFB3340-specific B cells.

In addition to detection of B cell activation across tissue sites, commensal-specific B cell tetramers enabled detection of early life B cell activation and the study of transgenerational immunity to commensal microbes in neonatal and adult mice. These tools will enable future investigation of early life humoral responses to natural colonization currently requiring models of maternal B cell or antibody deficiency and/or cross-fostering-based approaches.[8]

Finally, using a priori selection of SFB3340-specific B cells from the polyclonal repertoire, we performed focused BCR repertoire analyses, demonstrating that accrual of affinity enhancing antibody mutations occurs readily for commensal-specific B cells following *de novo* colonization, and this does not result in polyreactive antibody responses, but elevated antibody binding affinities for this commensal antigen. Targeted isolation of antigen-specific B cells allowed a direct demonstration of gut B cell selection, and future studies to incorporate elegant photoactivation and fate-mapping approaches will enable us to extend these studies to the resolution of singular PPs and even single GCs.[31]

Commensal-specific B cell tetramers will likely empower future investigation of the cellular heterogeneity in B cells responding to microbes in distinct experimental contexts, including heterologous immunity to commensal microbes during pathogen infection, malnutrition, autoimmunity, or within the tumor microenvironment. Key benefits of the B cell tetramer detection technology include the ability to precisely evaluate the cellular phenotype, isotype, kinetics, and polyclonal repertoire of antigen-specific B cells recognizing an endogenous protein antigen expressed at physiological concentrations and kinetics. Additionally, B cell tetramers are compatible with fluorescent reporters and transcription factor staining, enabling ready integration into established flow cytometric panels and approaches. Importantly, because B cell tetramers are not subject to major histocompatibility complex (MHC) restriction, they will enable comparisons of immunity to microbes across mouse haplotypes and across species, including humans and non-human primates.

In summary, here, we developed an approach with which to identify immunogenic antigens from commensal microbes, and subsequently utilized identified antigens to track commensal-specific B cell responses *ex vivo*, with the view that this approach will facilitate future studies of humoral immunity to commensal microbes, throughout the lifespan, across generations, and with anatomical resolution.

Limitations of the study

By virtue of being an affinity-based enrichment approach, phage display screening using polyclonal Ig is inherently biased toward identification of high-affinity antibody/antigen interactions. As such, this approach preferentially identifies antigens to which high-affinity antibodies are raised and may not identify antigens provoking low-affinity responses. Highly mutated and affine B cells contribute to gut homeostasis,[55] but the contribution of low-affinity responses remains to be determined. Future studies utilizing a panel of B cell tetramers akin to linking B cell receptor to antigen specificity through sequencing (LIBRA-seq),[56] could enable investigation of immune responses across a range of antibody affinities. While SFB elicits detectable serum antibody responses, this is not the case for all commensal microbes, and as such, serum antibodies may not be amenable for phage display screening of all target microbes. Phage display is restricted by the necessity for DNA encoded antigens, therefore limiting its utility for discovery of carbohydrate, lipid, or post-translationally modified proteins. Similarly, due to the size restriction of genomic DNA fragments used during library generation, detection of complex antigens derived from multimeric or conformational epitopes also represents a technical limitation of the approach, a limitation shared by other approaches for screening serum reactivity to short commensal-derived oligopeptides, including phage immunoprecipitation sequencing (PhIP-seq).[57] Utilization of phage display library screening to identify immunogenic antigens is amenable for culturable microbes, or those that can be isolated with relative purity under

gnotobiotic conditions. We have not systematically determined whether phage display libraries of sufficient size and complexity can be generated from diverse metagenomes to enable pan-commensal identification of immunogenic antigens. This is particularly pertinent to the B cell responses elicited by SFB, which include a non-specific component that is poorly understood and not captured using our current approaches. Generation of B cell tetramers is reliant upon stable expression of bacterial proteins in sufficient quantity to permit biotinylation and tetramerization, and as such, not all proteins may be amenable to being used as probes. Detection of antigen-specific B cells with tetramers is reliant on cell surface BCR/antigen interaction, currently negating the utility of these approaches to detect plasma cells due to low cell surface BCR expression. Ongoing efforts to generate commensal-specific BCR transgenic mice will likely circumnavigate these shortcomings.

STAR★METHODS

Detailed methods are provided in the online version of this paper and include the following:

- KEY RESOURCES TABLE
- RESOURCE AVAILABILITY
  - Lead Contact
  - Materials availability
  - Data and code availability
- EXPERIMENTAL MODEL AND STUDY PARTICIPANT DETAILS
  - Mouse strains
  - Bacterial strains and culture
  - Cell lines
- METHOD DETAILS
  - Construction of phage display library
  - Packaging of oligopeptide phage library
  - Phage Library Biopanning
  - Monoclonal Phage ELISA
  - Isolation of luminal antibodies
  - Enzyme-linked immunosorbent assay (ELISA)
  - ELISpot
  - Tetramer generation
  - De novo colonization with SFB containing feces
  - Quantification of fecal DNA
  - Flow cytometry
  - Isolation of leukocytes from tissues
  - Single-cell RNA-sequencing
  - Single-cell RNA-sequencing quality control and demultiplexing
  - Analysis of BCR sequence data
  - Recombinant antibody production
  - Site directed mutagenesis (SDM)
  - Recombinant antibody production for SDM
  - Biolayer Interferometry
  - Immunofluorescence staining
- QUANTIFICATION AND STATISTICAL ANALYSIS

SUPPLEMENTAL INFORMATION

Supplemental information can be found online at https://doi.org/10.1016/j.immuni.2024.04.014.

ACKNOWLEDGMENTS

We thank Drs. Meghan Koch, Jhimmy Talbot, Adam Lacy-Hulbert, Jessica Hamerman, Daniel Campbell, Allyson Byrd, and members of the Harrison Lab for discussions and critical reading of the manuscript. We thank Marion Pepper for *Cd4*^{Cre} x *Bcl6*$^{fl/fl}$ mice, Daniel Campbell for *Icos*$^{-/-}$ mice, and Meghan Koch for *Tcrbd*$^{-/-}$ mice. We thank Jessica Hamerman for serum from NZB/W mice. We thank Justin Taylor for technical guidance on B cell tetramer generation and usage. We also thank Benaroya Research Institute Cell and Tissue Analysis and Genomics Cores, particularly Caroline Stefani, Adam Wojno, Vivian Gersuk, Kimm O'Brien and Quynh-Anh Nguyen, as well as staff of the Benaroya Research Institute vivarium. We thank Jisun Paik for overseeing gnotobiotic experiments. We thank Michael Hust for provision of the pHORF3 vector and Dan Littman for sharing SFB-monocolonized feces. We thank the M.J. Murdock Charitable Trust for support of flow cytometry, histology, imaging, and genomics resources at Benaroya Research Institute. Experiment schematics were created with BioRender.com. This work was supported by Benaroya Research Institute, the Gut Immunity Program at Benaroya Research Institute, and the National Institutes of Health (R21AI171921). S.V. is a Washington Research Foundation Post-doctoral Fellow; T.M.O. is the recipient of a T32 CMB training grant (1T32GM136534) and a National Science Foundation GRFP fellowship (DGE-2140004); and O.J.H. was supported by NIH (R01AI158624).

AUTHOR CONTRIBUTIONS

S.V. performed experiments and analyzed the data. M.J.D. performed analysis of single-cell RNA sequencing and BCR repertoires. T.M.O., S.K., and J.C.L. aided with *in vivo* experiments and analyses. S.S. and A.T.M. performed antibody binding and affinity experiments and analyses. O.J.H. conceived the project, analyzed data, and wrote the manuscript with input from all co-authors.

DECLARATION OF INTERESTS

The authors declare no competing interests.

Received: October 12, 2023
Revised: February 7, 2024
Accepted: April 16, 2024
Published: May 8, 2024

REFERENCES

1. Kawamoto, S., Maruya, M., Kato, L.M., Suda, W., Atarashi, K., Doi, Y., Tsutsui, Y., Qin, H., Honda, K., Okada, T., et al. (2014). Foxp3(+) T cells regulate immunoglobulin a selection and facilitate diversification of bacterial species responsible for immune homeostasis. Immunity *41*, 152–165. https://doi.org/10.1016/j.immuni.2014.05.016.
2. Sutherland, D.B., Suzuki, K., and Fagarasan, S. (2016). Fostering of advanced mutualism with gut microbiota by Immunoglobulin A. Immunol. Rev. *270*, 20–31. https://doi.org/10.1111/imr.12384.
3. Ramanan, D., Sefik, E., Galván-Peña, S., Wu, M., Yang, L., Yang, Z., Kostic, A., Golovkina, T.V., Kasper, D.L., Mathis, D., et al. (2020). An Immunologic Mode of Multigenerational Transmission Governs a Gut Treg Setpoint. Cell *181*, 1276–1290.e13. https://doi.org/10.1016/j.cell.2020.04.030.
4. Rogier, E.W., Frantz, A.L., Bruno, M.E.C., Wedlund, L., Cohen, D.A., Stromberg, A.J., and Kaetzel, C.S. (2014). Secretory antibodies in breast milk promote long-term intestinal homeostasis by regulating the gut microbiota and host gene expression. Proc. Natl. Acad. Sci. USA *111*, 3074–3079. https://doi.org/10.1073/pnas.1315792111.
5. Bunker, J.J., Erickson, S.A., Flynn, T.M., Henry, C., Koval, J.C., Meisel, M., Jabri, B., Antonopoulos, D.A., Wilson, P.C., and Bendelac, A. (2017). Natural polyreactive IgA antibodies coat the intestinal microbiota. Science *358*, eaan6619. https://doi.org/10.1126/science.aan6619.
6. Bergqvist, P., Stensson, A., Lycke, N.Y., and Bemark, M. (2010). T cell-independent IgA class switch recombination is restricted to the GALT and occurs prior to manifest germinal center formation. J. Immunol. *184*, 3545–3553. https://doi.org/10.4049/jimmunol.0901895.
7. Zeng, M.Y., Cisalpino, D., Varadarajan, S., Hellman, J., Warren, H.S., Cascalho, M., Inohara, N., and Núñez, G. (2016). Gut Microbiota-Induced Immunoglobulin G Controls Systemic Infection by Symbiotic

Bacteria and Pathogens. Immunity *44*, 647–658. https://doi.org/10.1016/j.immuni.2016.02.006.

8. Koch, M.A., Reiner, G.L., Lugo, K.A., Kreuk, L.S.M., Stanbery, A.G., Ansaldo, E., Seher, T.D., Ludington, W.B., and Barton, G.M. (2016). Maternal IgG and IgA Antibodies Dampen Mucosal T Helper Cell Responses in Early Life. Cell *165*, 827–841. https://doi.org/10.1016/j.cell.2016.04.055.
9. Ansaldo, E., Farley, T.K., and Belkaid, Y. (2021). Control of Immunity by the Microbiota. Annu. Rev. Immunol. *39*, 449–479. https://doi.org/10.1146/annurev-immunol-093019-112348.
10. Fadlallah, J., Sterlin, D., Fieschi, C., Parizot, C., Dorgham, K., El Kafsi, H., Autaa, G., Ghillani-Dalbin, P., Juste, C., Lepage, P., et al. (2019). Synergistic convergence of microbiota-specific systemic IgG and secretory IgA. J. Allergy Clin. Immunol. *143*, 1575–1585.e4. https://doi.org/10.1016/j.jaci.2018.09.036.
11. Uchida, A.M., Boden, E.K., James, E.A., Shows, D.M., Konecny, A.J., and Lord, J.D. (2020). Escherichiacoli-Specific CD4+ T Cells Have Public T-Cell Receptors and Low Interleukin 10 Production in Crohn's Disease. Cell. Mol. Gastroenterol. Hepatol. *10*, 507–526. https://doi.org/10.1016/j.jcmgh.2020.04.013.
12. Martin, J.C., Chang, C., Boschetti, G., Ungaro, R., Giri, M., Grout, J.A., Gettler, K., Chuang, L.S., Nayar, S., Greenstein, A.J., et al. (2019). Single-Cell Analysis of Crohn's Disease Lesions Identifies a Pathogenic Cellular Module Associated with Resistance to Anti-TNF Therapy. Cell *178*, 1493–1508.e20. https://doi.org/10.1016/j.cell.2019.08.008.
13. Ansaldo, E., Slayden, L.C., Ching, K.L., Koch, M.A., Wolf, N.K., Plichta, D.R., Brown, E.M., Graham, D.B., Xavier, R.J., Moon, J.J., et al. (2019). Akkermansia muciniphila induces intestinal adaptive immune responses during homeostasis. Science *364*, 1179–1184. https://doi.org/10.1126/science.aaw7479.
14. Atarashi, K., Tanoue, T., Shima, T., Imaoka, A., Kuwahara, T., Momose, Y., Cheng, G., Yamasaki, S., Saito, T., Ohba, Y., et al. (2011). Induction of colonic regulatory T cells by indigenous Clostridium species. Science *331*, 337–341. https://doi.org/10.1126/science.1198469.
15. Atarashi, K., Tanoue, T., Oshima, K., Suda, W., Nagano, Y., Nishikawa, H., Fukuda, S., Saito, T., Narushima, S., Hase, K., et al. (2013). Treg induction by a rationally selected mixture of Clostridia strains from the human microbiota. Nature *500*, 232–236. https://doi.org/10.1038/nature12331.
16. Doron, I., Mesko, M., Li, X.V., Kusakabe, T., Leonardi, I., Shaw, D.G., Fiers, W.D., Lin, W.Y., Bialt-DeCelie, M., Román, E., et al. (2021). Mycobiota-induced IgA antibodies regulate fungal commensalism in the gut and are dysregulated in Crohn's disease. Nat. Microbiol. *6*, 1493–1504. https://doi.org/10.1038/s41564-021-00983-z.
17. Xu, M., Pokrovskii, M., Ding, Y., Yi, R., Au, C., Harrison, O.J., Galan, C., Belkaid, Y., Bonneau, R., and Littman, D.R. (2018). c-MAF-dependent regulatory T cells mediate immunological tolerance to a gut pathobiont. Nature *554*, 373–377. https://doi.org/10.1038/nature25500.
18. Chai, J.N., Peng, Y., Rengarajan, S., Solomon, B.D., Ai, T.L., Shen, Z., Perry, J.S.A., Knoop, K.A., Tanoue, T., Narushima, S., et al. (2017). Helicobacter species are potent drivers of colonic T cell responses in homeostasis and inflammation. Sci. Immunol. *2*, aal5068. https://doi.org/10.1126/sciimmunol.aal5068.
19. Belkaid, Y., and Harrison, O.J. (2017). Homeostatic Immunity and the Microbiota. Immunity *46*, 562–576. https://doi.org/10.1016/j.immuni.2017.04.008.
20. Ivanov, I.I., Atarashi, K., Manel, N., Brodie, E.L., Shima, T., Karaoz, U., Wei, D., Goldfarb, K.C., Santee, C.A., Lynch, S.V., et al. (2009). Induction of intestinal Th17 cells by segmented filamentous bacteria. Cell *139*, 485–498. https://doi.org/10.1016/j.cell.2009.09.033.
21. Bunker, J.J., Flynn, T.M., Koval, J.C., Shaw, D.G., Meisel, M., McDonald, B.D., Ishizuka, I.E., Dent, A.L., Wilson, P.C., Jabri, B., et al. (2015). Innate and Adaptive Humoral Responses Coat Distinct Commensal Bacteria with Immunoglobulin A. Immunity *43*, 541–553. https://doi.org/10.1016/j.immuni.2015.08.007.
22. Gaboriau-Routhiau, V., Rakotobe, S., Lécuyer, E., Mulder, I., Lan, A., Bridonneau, C., Rochet, V., Pisi, A., De Paepe, M., Brandi, G., et al. (2009). The key role of segmented filamentous bacteria in the coordinated maturation of gut helper T cell responses. Immunity *31*, 677–689. https://doi.org/10.1016/j.immuni.2009.08.020.
23. Talham, G.L., Jiang, H.Q., Bos, N.A., and Cebra, J.J. (1999). Segmented filamentous bacteria are potent stimuli of a physiologically normal state of the murine gut mucosal immune system. Infect. Immun. *67*, 1992–2000. https://doi.org/10.1128/IAI.67.4.1992-2000.1999.
24. Umesaki, Y., Setoyama, H., Matsumoto, S., Imaoka, A., and Itoh, K. (1999). Differential roles of segmented filamentous bacteria and clostridia in development of the intestinal immune system. Infect. Immun. *67*, 3504–3511. https://doi.org/10.1128/IAI.67.7.3504-3511.1999.
25. Palm, N.W., de Zoete, M.R., Cullen, T.W., Barry, N.A., Stefanowski, J., Hao, L., Degnan, P.H., Hu, J., Peter, I., Zhang, W., et al. (2014). Immunoglobulin A coating identifies colitogenic bacteria in inflammatory bowel disease. Cell *158*, 1000–1010. https://doi.org/10.1016/j.cell.2014.08.006.
26. Wu, H.J., Ivanov, I.I., Darce, J., Hattori, K., Shima, T., Umesaki, Y., Littman, D.R., Benoist, C., and Mathis, D. (2010). Gut-residing segmented filamentous bacteria drive autoimmune arthritis via T helper 17 cells. Immunity *32*, 815–827. https://doi.org/10.1016/j.immuni.2010.06.001.
27. Lee, Y.K., Menezes, J.S., Umesaki, Y., and Mazmanian, S.K. (2011). Proinflammatory T-cell responses to gut microbiota promote experimental autoimmune encephalomyelitis. Proc. Natl. Acad. Sci. USA *108* (*Suppl 1*), 4615–4622. https://doi.org/10.1073/pnas.1000082107.
28. Yang, Y., Torchinsky, M.B., Gobert, M., Xiong, H., Xu, M., Linehan, J.L., Alonzo, F., Ng, C., Chen, A., Lin, X., et al. (2014). Focused specificity of intestinal TH17 cells towards commensal bacterial antigens. Nature *510*, 152–156. https://doi.org/10.1038/nature13279.
29. Kau, A.L., Planer, J.D., Liu, J., Rao, S., Yatsunenko, T., Trehan, I., Manary, M.J., Liu, T.C., Stappenbeck, T.S., Maleta, K.M., et al. (2015). Functional characterization of IgA-targeted bacterial taxa from undernourished Malawian children that produce diet-dependent enteropathy. Sci. Transl. Med. *7*, 276ra24. https://doi.org/10.1126/scitranslmed.aaa4877.
30. Vujkovic-Cvijin, I., Welles, H.C., Ha, C.W.Y., Huq, L., Mistry, S., Brenchley, J.M., Trinchieri, G., Devkota, S., and Belkaid, Y. (2022). The systemic anti-microbiota IgG repertoire can identify gut bacteria that translocate across gut barrier surfaces. Sci. Transl. Med. *14*, eabl3927. https://doi.org/10.1126/scitranslmed.abl3927.
31. Nowosad, C.R., Mesin, L., Castro, T.B.R., Wichmann, C., Donaldson, G.P., Araki, T., Schiepers, A., Lockhart, A.A.K., Bilate, A.M., Mucida, D., et al. (2020). Tunable dynamics of B cell selection in gut germinal centres. Nature *588*, 321–326. https://doi.org/10.1038/s41586-020-2865-9.
32. Chen, H., Zhang, Y., Ye, A.Y., Du, Z., Xu, M., Lee, C.S., Hwang, J.K., Kyritsis, N., Ba, Z., Neuberg, D., et al. (2020). BCR selection and affinity maturation in Peyer's patch germinal centres. Nature *582*, 421–425. https://doi.org/10.1038/s41586-020-2262-4.
33. Lindner, C., Wahl, B., Föhse, L., Suerbaum, S., Macpherson, A.J., Prinz, I., and Pabst, O. (2012). Age, microbiota, and T cells shape diverse individual IgA repertoires in the intestine. J. Exp. Med. *209*, 365–377. https://doi.org/10.1084/jem.20111980.
34. Rollenske, T., Burkhalter, S., Muerner, L., von Gunten, S., Lukasiewicz, J., Wardemann, H., and Macpherson, A.J. (2021). Parallelism of intestinal secretory IgA shapes functional microbial fitness. Nature *598*, 657–661. https://doi.org/10.1038/s41586-021-03973-7.
35. Meyer, T., Schirrmann, T., Frenzel, A., Miethe, S., Stratmann-Selke, J., Gerlach, G.F., Strutzberg-Minder, K., Dübel, S., and Hust, M. (2012). Identification of immunogenic proteins and generation of antibodies against Salmonella Typhimurium using phage display. BMC Biotechnol. *12*, 29. https://doi.org/10.1186/1472-6750-12-29.
36. Connor, D.O., Zantow, J., Hust, M., Bier, F.F., and von Nickisch-Rosenegk, M. (2016). Identification of Novel Immunogenic Proteins of Neisseria gonorrhoeae by Phage Display. PLoS One *11*, e0148986. https://doi.org/10.1371/journal.pone.0148986.

37. Krishnamurty, A.T., Thouvenel, C.D., Portugal, S., Keitany, G.J., Kim, K.S., Holder, A., Crompton, P.D., Rawlings, D.J., and Pepper, M. (2016). Somatically Hypermutated Plasmodium-Specific IgM(+) Memory B Cells Are Rapid, Plastic, Early Responders upon Malaria Rechallenge. Immunity *45*, 402–414. https://doi.org/10.1016/j.immuni.2016.06.014.

38. Allie, S.R., Bradley, J.E., Mudunuru, U., Schultz, M.D., Graf, B.A., Lund, F.E., and Randall, T.D. (2019). The establishment of resident memory B cells in the lung requires local antigen encounter. Nat. Immunol. *20*, 97–108. https://doi.org/10.1038/s41590-018-0260-6.

39. Hust, M., Meysing, M., Schirrmann, T., Selke, M., Meens, J., Gerlach, G.F., and Dübel, S. (2006). Enrichment of open reading frames presented on bacteriophage M13 using hyperphage. BioTechniques *41*, 335–342. https://doi.org/10.2144/000112225.

40. Rondot, S., Koch, J., Breitling, F., and Dübel, S. (2001). A helper phage to improve single-chain antibody presentation in phage display. Nat. Biotechnol. *19*, 75–78. https://doi.org/10.1038/83567.

41. Tafuri, A., Shahinian, A., Bladt, F., Yoshinaga, S.K., Jordana, M., Wakeham, A., Boucher, L.M., Bouchard, D., Chan, V.S., Duncan, G., et al. (2001). ICOS is essential for effective T-helper-cell responses. Nature *409*, 105–109. https://doi.org/10.1038/35051113.

42. Hollister, K., Kusam, S., Wu, H., Clegg, N., Mondal, A., Sawant, D.V., and Dent, A.L. (2013). Insights into the role of Bcl6 in follicular Th cells using a new conditional mutant mouse model. J. Immunol. *191*, 3705–3711. https://doi.org/10.4049/jimmunol.1300378.

43. Taylor, J.J., Martinez, R.J., Titcombe, P.J., Barsness, L.O., Thomas, S.R., Zhang, N., Katzman, S.D., Jenkins, M.K., and Mueller, D.L. (2012). Deletion and anergy of polyclonal B cells specific for ubiquitous membrane-bound self-antigen. J. Exp. Med. *209*, 2065–2077. https://doi.org/10.1084/jem.20112272.

44. Vergani, S., Muleta, K.G., Da Silva, C., Doyle, A., Kristiansen, T.A., Sodini, S., Krausse, N., Montano, G., Kotarsky, K., Nakawesi, J., et al. (2022). A self-sustaining layer of early-life-origin B cells drives steady-state IgA responses in the adult gut. Immunity *55*, 1829–1842.e6. https://doi.org/10.1016/j.immuni.2022.08.018.

45. Jiang, H.Q., Bos, N.A., and Cebra, J.J. (2001). Timing, localization, and persistence of colonization by segmented filamentous bacteria in the neonatal mouse gut depend on immune status of mothers and pups. Infect. Immun. *69*, 3611–3617. https://doi.org/10.1128/IAI.69.6.3611-3617.2001.

46. Esterházy, D., Canesso, M.C.C., Mesin, L., Muller, P.A., de Castro, T.B.R., Lockhart, A., ElJalby, M., Faria, A.M.C., and Mucida, D. (2019). Compartmentalized gut lymph node drainage dictates adaptive immune responses. Nature *569*, 126–130. https://doi.org/10.1038/s41586-019-1125-3.

47. Mayer, J.U., Brown, S.L., MacDonald, A.S., and Milling, S.W. (2020). Defined Intestinal Regions Are Drained by Specific Lymph Nodes That Mount Distinct Th1 and Th2 Responses Against Schistosoma mansoni Eggs. Front. Immunol. *11*, 592325. https://doi.org/10.3389/fimmu.2020.592325.

48. Houston, S.A., Cerovic, V., Thomson, C., Brewer, J., Mowat, A.M., and Milling, S. (2016). The lymph nodes draining the small intestine and colon are anatomically separate and immunologically distinct. Mucosal Immunol. *9*, 468–478. https://doi.org/10.1038/mi.2015.77.

49. Sano, T., Huang, W., Hall, J.A., Yang, Y., Chen, A., Gavzy, S.J., Lee, J.Y., Ziel, J.W., Miraldi, E.R., Domingos, A.I., et al. (2015). An IL-23R/IL-22 Circuit Regulates Epithelial Serum Amyloid A to Promote Local Effector Th17 Responses. Cell *163*, 381–393. https://doi.org/10.1016/j.cell.2015.08.061.

50. Raso, F., Liu, S., Simpson, M.J., Barton, G.M., Mayer, C.T., Acharya, M., Muppidi, J.R., Marshak-Rothstein, A., and Reboldi, A. (2023). Antigen receptor signaling and cell death resistance controls intestinal humoral response zonation. Immunity *56*, 2373–2387.e8. https://doi.org/10.1016/j.immuni.2023.08.018.

51. Belkaid, Y., and Hand, T.W. (2014). Role of the microbiota in immunity and inflammation. Cell *157*, 121–141. https://doi.org/10.1016/j.cell.2014.03.011.

52. Lécuyer, E., Rakotobe, S., Lengliné-Garnier, H., Lebreton, C., Picard, M., Juste, C., Fritzen, R., Eberl, G., McCoy, K.D., Macpherson, A.J., et al. (2014). Segmented filamentous bacterium uses secondary and tertiary lymphoid tissues to induce gut IgA and specific T helper 17 cell responses. Immunity *40*, 608–620. https://doi.org/10.1016/j.immuni.2014.03.009.

53. Bang, Y.J., Hu, Z., Li, Y., Gattu, S., Ruhn, K.A., Raj, P., Herz, J., and Hooper, L.V. (2021). Serum amyloid A delivers retinol to intestinal myeloid cells to promote adaptive immunity. Science *373*, eabf9232. https://doi.org/10.1126/science.abf9232.

54. Hand, T.W., and Reboldi, A. (2021). Production and Function of Immunoglobulin A. Annu. Rev. Immunol. *39*, 695–718. https://doi.org/10.1146/annurev-immunol-102119-074236.

55. Wei, M., Shinkura, R., Doi, Y., Maruya, M., Fagarasan, S., and Honjo, T. (2011). Mice carrying a knock-in mutation of Aicda resulting in a defect in somatic hypermutation have impaired gut homeostasis and compromised mucosal defense. Nat. Immunol. *12*, 264–270. https://doi.org/10.1038/ni.1991.

56. Setliff, I., Shiakolas, A.R., Pilewski, K.A., Murji, A.A., Mapengo, R.E., Janowska, K., Richardson, S., Oosthuysen, C., Raju, N., Ronsard, L., et al. (2019). High-Throughput Mapping of B Cell Receptor Sequences to Antigen Specificity. Cell *179*, 1636–1646.e15. https://doi.org/10.1016/j.cell.2019.11.003.

57. Andreu-Sánchez, S., Bourgonje, A.R., Vogl, T., Kurilshikov, A., Leviatan, S., Ruiz-Moreno, A.J., Hu, S., Sinha, T., Vich Vila, A., Klompus, S., et al. (2023). Phage display sequencing reveals that genetic, environmental, and intrinsic factors influence variation of human antibody epitope repertoire. Immunity *56*, 1376–1392.e8. https://doi.org/10.1016/j.immuni.2023.04.003.

58. Hao, Y., Hao, S., Andersen-Nissen, E., Mauck, W.M., 3rd, Zheng, S., Butler, A., Lee, M.J., Wilk, A.J., Darby, C., Zager, M., et al. (2021). Integrated analysis of multimodal single-cell data. Cell *184*, 3573–3587.e29. https://doi.org/10.1016/j.cell.2021.04.048.

59. Gupta, N.T., Vander Heiden, J.A., Uduman, M., Gadala-Maria, D., Yaari, G., and Kleinstein, S.H. (2015). Change-O: a toolkit for analyzing large-scale B cell immunoglobulin repertoire sequencing data. Bioinformatics *31*, 3356–3358. https://doi.org/10.1093/bioinformatics/btv359.

60. Nixon, K.C. (1999). The Parsimony Ratchet, a New Method for Rapid Parsimony Analysis. Cladistics *15*, 407–414. https://doi.org/10.1111/j.1096-0031.1999.tb00277.x.

61. Schliep, K.P. (2011). phangorn: phylogenetic analysis in R. Bioinformatics *27*, 592–593. https://doi.org/10.1093/bioinformatics/btq706.

STAR★METHODS

KEY RESOURCES TABLE

REAGENT or RESOURCE	SOURCE	IDENTIFIER
Antibodies		
Anti-B220 BUV737 (Clone: RA3-6B2)	BD Biosciences	Cat# 612838; RRID:AB_2870160
Anti-CD95 BUV805 (Clone: Jo2)	BD Biosciences	Cat# 741968; RRID:AB_2871273
Anti-GL7 Pacific Blue (clone: GL7)	BioLegend	Cat# 144614; RRID:AB_2563291
Anti-CD138 BV650 (clone: 281-20)	BioLegend	Cat# 142518; RRID:AB_2650927
Anti-IgD BV510 (clone: 11-26c.2a)	BioLegend	Cat# 405723; RRID:AB_2562742
Anti-IgM BV711 (clone: II/41)	BD Biosciences	Cat# 743327; RRID:AB_2741428
Anti-IgA FITC	SouthernBiotech	Cat# 1040-02; RRID: AB_2794370
Anti-IgG1 PerCP/Cy5.5 (clone: RMG1-1)	BioLegend	Cat# 406612; RRID:AB_2562000
Anti-IgG2b PE/Cy7 (clone: RMG2b-1)	BioLegend	Cat# 406714; RRID:AB_2750280
Anti-CD38 AF700 (clone: 90)	BioLegend	Cat# 102742; RRID:AB_2890672
Anti-CD90.2 BV785 (clone: 30-H12)	BioLegend	Cat# 105331; RRID:AB_2562900
Anti-F4/80 BV785 (clone: BM8)	BioLegend	Cat# 123141; RRID:AB_2563667
Anti-CD11c BV785 (clone: N418)	BioLegend	Cat# 117336; RRID:AB_2565268
Anti-Ly-6G BV785 (clone 1A8)	BioLegend	Cat# 127645; RRID:AB_2566317
Anti-CD45 APC-eFluor780 (clone: 30-F11)	Thermo Scientific	Cat# 47-0451-82; RRID: AB_1548781
Anti-Ovalbumin (clone: F2-3.58)	BioXCell	Cat# RT0267; RRID: AB_2651130
Anti-Bovine Serum Albumin	SouthernBiotech	Cat# 2079-01; RRID: AB_2795778
Anti-LPS (clone: SLP-32)	Sigma Aldrich	Cat# SAB4200882
Unlabeled Goat Anti-Mouse IgA	SouthernBiotech	Cat# 1040-01; RRID:AB_2314669
Unlabeled Goat Anti-Mouse IgG	SouthernBiotech	Cat# 1030-01; RRID:AB_2794290
Goat Anti-Mouse IgA-HRP	SouthernBiotech	Cat# 1040-05; RRID:AB_2714213
Goat Anti-Mouse IgG1-HRP	SouthernBiotech	Cat# 1070-05; RRID:AB_2650509
Goat Anti-Mouse IgG2b-HRP	SouthernBiotech	Cat# 1090-05; RRID:AB_2794521
Goat Anti-Mouse IgE-HRP	SouthernBiotech	Cat# 1110-05; RRID:AB_2794604
Goat Anti-Mouse IgM-HRP	Jackson Immunoresearch	Cat# 115-035-020; RRID:AB_2338502
Goat Anti-Mouse IgG2c-HRP	Jackson Immunoresearch	Cat# 115-005-208; RRID:AB_2338464
Goat Anti-Mouse IgG3-HRP	Jackson Immunoresearch	Cat# 115-035-209; RRID:AB_2338517
M13 Phage coat protein Polyclonal Antibody	Thermo Scientific	Cat# PA1-26758; RRID:AB_795743
Mouse Anti-Human IgG R718	BD Biosciences	Cat # 751917; RRID: AB_2917040
Anti-CD326 Alexa Fluor® 488 (clone G8.8)	BioLegend	Cat # 118210; RRID:AB_1134099
Goat Anti-Human IgG-HRP	SouthernBiotech	Cat #2040-05; RRID:AB_2795644
TotalSeq™-C0301 anti-mouse Hashtag 1 Antibody	BioLegend	Cat #155861; RRID:AB_2800693
TotalSeq™-C0302 anti-mouse Hashtag 2 Antibody	BioLegend	Cat #155863; RRID:AB_2800694
TotalSeq™-C0303 anti-mouse Hashtag 3 Antibody	BioLegend	Cat #155865; RRID:AB_2800695
TotalSeq™-C0304 anti-mouse Hashtag 4 Antibody	BioLegend	Cat #155867; RRID:AB_2800696
TotalSeq™-C0305 anti-mouse Hashtag 5 Antibody	BioLegend	Cat #155869; RRID:AB_2800697
TotalSeq™-C0306 anti-mouse Hashtag 6 Antibody	BioLegend	Cat #155871; RRID:AB_2819910

(*Continued on next page*)

Continued

REAGENT or RESOURCE	SOURCE	IDENTIFIER
TotalSeq™-C0307 anti-mouse Hashtag 7 Antibody	BioLegend	Cat #155873; RRID:AB_2819911
TotalSeq™-C0308 anti-mouse Hashtag 8 Antibody	BioLegend	Cat #155875; RRID:AB_2819912
TotalSeq™-C0309 anti-mouse Hashtag 9 Antibody	BioLegend	Cat #155877; RRID:AB_2819913
TotalSeq™-C0310 anti-mouse Hashtag 10 Antibody	BioLegend	Cat #155879; RRID:AB_2819914
Anti-SFB3340 (V_H1-53-UA)	This paper	N/A
Anti-SFB3340 (V_H1-53-N1)	This paper	N/A
Anti-SFB3340 (V_H1-53-N5)	This paper	N/A
Anti-SFB3340 (V_H1-53-N10)	This paper	N/A
Anti-SFB3340 (V_H1-53-CARYDYAWFAYW)	This paper	N/A
Anti-SFB3340 (V_H1-53-CARHDYAWFAYW)	This paper	N/A
Anti-SFB3340 (V_H1-53-CARGDYAWFAYW)	This paper	N/A
Anti-SFB3340 (V_H1-53-CARDDYDWFAYW)	This paper	N/A
Anti-SFB3340 (V_H1-53-CARDDYAGFAYW)	This paper	N/A
Anti-SFB3340 (V_H1-53-CARDDYDGFAYW)	This paper	N/A
Anti-SFB3340 (V_H1-76-UA)	This paper	N/A
Anti-SFB3340 (V_H1-76-N1)	This paper	N/A
Anti-SFB3340 (V_H1-76-N14)	This paper	N/A
Anti-SFB3340 (V_H1-76-N6)	This paper	N/A
Anti-SFB3340 (V_H1-76-N9)	This paper	N/A
Anti-SFB3340 (V_H1-76-N11)	This paper	N/A
Anti-SFB3340 (V_H1-76-N38)	This paper	N/A
Anti-SFB3340 (V_H1-76-CARSHYYGSSYWYFDVW)	This paper	N/A
Anti-SFB3340 (V_H1-76-CARGHYYGSSYWYFDVW)	This paper	N/A
Anti-SFB3340 (V_H1-76-CARAYYYGSSYWYFDVW)	This paper	N/A
Anti-SFB3340 (V_H1-76-CARSYYYGSSYWYFDVW)	This paper	N/A
Anti-SFB3340 (V_H1-76-CARAHYYGNSYWYFDVW)	This paper	N/A
Bacterial Strains		
Stbl3 cells	Invitrogen	Cat# C737303
TG1 competent cells	Lucigen	Cat# 60502-2
Segmented Filamentous Bacteria	Prof. Dan Littman, NYU Langone Health	
Chemicals, peptides, and recombinant proteins		
Liberase TL	Sigma Aldrich	Cat# 5401020001
DNase I	Sigma Aldrich	Cat# DN25-5G
EDTA	VWR	Cat# 45001-122
DL-Dithiothreitol (DTT)	Sigma Aldrich	Cat# D0632-5G
Recombinant SFB3340 protein	GenScript	N/A
Decoy peptide	GenScript	N/A
Polybead Microspheres 15.00 um	Polysciences	Cat# 183285
TMB substrate	BD Biosciences	Cat# 555214
AEC Substrate Kit, Peroxidase (HRP)	Vector Laboratories	Cat# SK-4200
Hyperphage M13 KO7ΔpIII	Progen Biotechnik	Cat# PRHYPE

(*Continued on next page*)

Continued

REAGENT or RESOURCE	SOURCE	IDENTIFIER
Thermo Scientific EZ Link Plus Activated Peroxidase Kit	Thermo Scientific	Cat# 31489
Streptavidin-RPE	Agilent	Cat# PJRS25-1
Streptavidin, Alexa Fluor™ 680 conjugate	Invitrogen	Cat# S21378
Protein G Sepharose 4 Fast Flow, 5 ml	Cytiva	Cat# GE17-0618-01
Percoll	GE Healthcare	Cat# GE17-0891-09
LIVE/DEAD™ Fixable Blue Dead Cell Stain Kit, for UV excitation	Thermo Scientific	Cat# L34962
Super Bright Complete Staining Buffer, eBioscience	Thermo Scientific	Cat# SB-4401-75
Applied Biosystems PowerUp SYBR Green Master Mix	Thermo Scientific	Cat# A25742
Bolt™ 4-12% Bis-Tris Plus Gels, 15-well	Thermo Scientific	Cat# NW04125BOX
Invitrogen Novex 20X Bolt MES SDS Running Buffer	Thermo Scientific	Cat# B0002
UltraComp eBeads™ Plus Compensation Beads	Thermo Scientific	Cat# 01-3333-42
Arc™ Amine Reactive Compensation Bead Kit	Thermo Scientific	Cat# A10346
Expi293™ Expression Medium	Thermo Scientific	Cat# A1435101
ExpiFectamine™ 293 Transfection Kit:	Thermo Scientific	Cat# A14524
Phusion High Fidelity DNA Polymerase	Thermo Scientific	Cat# F530L
DyLight™ 594 NHS Ester	Thermo Scientific	Cat# 46413
Molecular Probes ProLong Gold Antifade Mountant	Thermo Scientific	Cat# P36930
Critical Commercial Assays		
QIAprep Spin Miniprep Kit	Qiagen	Cat# 27106
Quick-DNA Fecal/Soil Microbe DNA Miniprep Kit	Zymo Research	Cat# D6010
BD Cytofix/Cytoperm	BD Biosciences	Cat# 554655
Fast DNA End Repair Kit	Thermo Scientific	Cat# K0771
DNA Clean & Concentrator-5, Capped Columns	Zymo Research	Cat# D4013
Chromium Next GEM Single Cell 5′ Reagent Kits	10X Genomics	Cat# CG000592
Deposited data		
Single-cell RNA-seq data	This paper	GEO: GSE245084
Experimental models: Cell lines		
Expi293F™ Cells	Thermo Scientific	Cat# A14527
Recombinant DNA		
TOPO™ TA Cloning™ Kit	Thermo Scientific	Cat# K450002
AbVec1.1-IGKC	Addgene	Cat# 80796
AbVec2.0-IGHG1	Addgene	Cat# 80795
pHORF3 phagemid	Meyer et al.[35]	N/A
Experimental models: Organisms/strains		
C57bl/6j	The Jackson Laboratory	RRID:IMSR_JAX:000664
Cd4^{Cre} x *Bcl6*$^{fl/fl}$	Dr. Marion Pepper, University of Washington	RRID:IMSR_JAX:017336,
Tcrbd$^{-/-}$	Dr. Meghan Koch, Fred Hutch Cancer Center	RRID:IMSR_JAX:002118, RRID:IMSR_JAX:002120
C57BL/6NTac	Taconic Biosciences	RRID:IMSR_TAC:B6

(*Continued on next page*)

Continued

REAGENT or RESOURCE	SOURCE	IDENTIFIER
Icos$^{-/-}$	Dr. Daniel Campbell, Benaroya Research Institute	RRID:IMSR_JAX:004859
Rag2$^{-/-}$*Il2rg*$^{-/-}$	Envigo	Strain: B6;129-Rag2tm1FwaIl2rgtm1Rsky/DwlHsd
Software and algorithms		
FlowJo 10 Software	Treestar	https://www.flowjo.com; FlowJo (RRID:SCR_008520)
GraphPad Prism 10	GraphPad Software	https://www.graphpad.com; RRID:SCR_002798
ImageJ	ImageJ	https://imagej.net/ij/; RRID:SCR_003070
Adobe Illustrator	Adobe Systems	https://www.adobe.com; RRID:SCR_010279
Biorender	Biorender	https://www.biorender.com; RRID:SCR_018361
SnapGene	Snapgene	https://www.snapgene.com/; RRID:SCR_015052
Cell Ranger v. 6.1.1	10x Genomics	https://www.10xgenomics.com; RRID:SCR_017344
Seurat Toolkit v. 4.3	Hao et al.[58]	https://satijalab.org/seurat/get_started.html; RRID:SCR_016341
Change-O	Gupta et al.[59]	https://changeo.readthedocs.io; RRID:SCR_023986
Shazam	Gupta et al.[59]	https://cran.r-project.org/web/packages/shazam/index.html; RRID:SCR_024301
Phangorn	Schliep[60]	https://cran.r-project.org/web/packages/phangorn/index.html; RRID:SCR_017302

RESOURCE AVAILABILITY

Lead Contact

Further information and requests for resources and reagents should be directed to and will be fulfilled by the lead contact, Oliver J. Harrison (oharrison@benaroyaresearch.org).

Materials availability

Mouse lines used in this study can be purchased, produced by breeding commercially available strains, or obtained from the donating lab(s) referenced. All additional reagents developed in the study will be made available by the lead contact.

Data and code availability

The single-cell RNA sequencing data have been deposited in GEO at NCBI with accession number GSE245084. All original code generated to analyze scRNA and VDJ sequencing are available from Benaroya Research Institute Github - https://github.com/BenaroyaResearch/Verma_Harrison_SFB_B_cells_2024

EXPERIMENTAL MODEL AND STUDY PARTICIPANT DETAILS

Mouse strains

Wild-type (WT) C57BL/6 Specific Pathogen Free (SPF) mice were purchased from Taconic Biosciences and Jackson Laboratories. *Rag2*$^{-/-}$*Il2rg*$^{-/-}$ (R2G2) mice were purchased from Envigo and colonized with SFB using feces from Taconic B6 mice. *Cd4*^{Cre} x *Bcl6*$^{fl/fl}$, *Icos*$^{-/-}$ and *Tcrbd*$^{-/-}$ mice were generously provided by Marion Pepper (University of Washington), Daniel Campbell (Benaroya Research Institute), and Meghan Koch (Fred Hutchinson Cancer Center), respectively. All specified pathogen free (SPF) mice were maintained at Benaroya Research Institute, and experiments were approved by the Institutional Animal Care and Use Committee of Benaroya Research Institute and performed according to their guidelines. Germ-free mice and SFB-monocolonized mice were housed in the University of Washington Gnotobiotic Animal Core. All experimental procedures were approved by the Institutional Animal Care and Use Committee at the University of Washington and performed according to their guidelines. Mice used in experiments were between 6 and 12 weeks of age at time of sacrifice unless specified. Both female and male mice were used for experiments.

Bacterial strains and culture

Segmented Filamentous Bacteria used for monocolonization of gnotobiotic mice were stored at -80 °C until use. Frozen fecal pellets were resuspended in sterile PBS and clarified by centrifuging the bacterial pellet at 300g, prior to oral gavage. For colonization of SPF mice using SFB-containing flora, fresh fecal pellets were collected from *Rag2*$^{-/-}$*Il2rg*$^{-/-}$ mice and processed as above. TG1 strain of *E.coli* used for phage display generation were cultured in or on 2 x YT (1.6% (w/v) tryptone, 1% (w/v) yeast extract, 0.05% (w/v) NaCl, 1.2% (w/v) agar) in some cases supplemented with 100 mM glucose and 100 μg/mL ampicillin (2× YT-GA), or 100 μg/mL ampicillin and 50 μg/mL kanamycin (2× YT-AK). Stbl3 strain of *E.coli* was used for cloning and cultured in Luria Broth supplemented with 100 μg/mL ampicillin.

Cell lines

Expi293F cells used for monoclonal antibody production were cultured in Expi293 Expression Medium following the manufacturer's instructions.

METHOD DETAILS

Construction of phage display library

Genomic DNA was purified from the feces of SFB-monocolonized mice using DNeasy PowerSoil Pro Kit according to the manufacturer's instructions. Purified DNA was fragmented by sonication using a Covaris M220 Focused-ultrasonicator. Fragmented DNA was analyzed on 1% agarose gels to ensure fragment sizes between 200 and 600 bp. Cohesive ends were blunted and repaired using Fast DNA End Repair Kit (Thermo Scientific). DNA was purified using a spin column (Zymo Research). The libraries were generated by blunt-end cloning of 1,200 ng fragmented DNA into 1,000 ng PmeI linearized and dephosphorylated pHORF3 library vector (a gift from Michael Hust, Technische Universität Braunschweig) (16 hr at 16 °C, T4 DNA Ligase, NEB). The ligation reaction was purified and transformed into TG1 bacteria (Lucigen) by electroporation (1.8 kV, MicroPulser, BioRad). After 1 hr of incubation at 37 °C and 600 rpm in 1 mL SOC medium, transformation rates were determined by plating dilutions on 2× YT agar (1.6% (w/v) tryptone, 1% (w/v) yeast extract, 0.05% (w/v) NaCl, 1.2% (w/v) agar) supplemented with 100 mM glucose and 100 μg/mL ampicillin (2× YT-GA). Cells were plated on 2× YT-GA agar plates (25 × 25 cm) and incubated at 37°C overnight. The cells were scraped using 20 mL of 2× TY medium, and stored at −80 °C in 20% (v/v) glycerol. Insert rates and mean insert sizes were determined by colony PCR and agarose gel electrophoresis of randomly analyzed colonies (n=24).

Packaging of oligopeptide phage library

Four hundred mL of 2×TY-GA medium were inoculated with glycerol stock of library to an OD600 < 0.1 and incubated at 37 °C and 250 rpm until an OD600 of 0.5 was reached. In order to complement the missing coat proteins and ensure enrichment for ORFs, 25 mL of the culture were infected with a 20-fold excess i.e. 2.5 × 10^{11} colony forming units (c.f.u.) of the M13K07ΔgIII helper phage "Hyperphage"(Progen) for 30 min at 37 °C. The infected cells were incubated for another 30 min at 37 °C and 250 rpm to express antibiotics resistance. The cells were pelleted (3,200× g, 10 min) and subsequently resuspended in 400 mL 2× YT medium supplemented with 100 μg/mL ampicillin and 50 μg/mL kanamycin (2× YT-AK). Oligopeptide phage particles were produced for 24 hr at 30 °C and 250 rpm. The supernatant containing phage particles were precipitated at 4 °C overnight after adding 1/5 volume precipitation buffer (20% (w/v) PEG 6,000, 2.5 M NaCl). The precipitated phage particles were pelleted for 1 hr at 10,000× g and 4 °C (Sorvall Centrifuge) and resuspended in 10 mL of 1X PBS. A second precipitation step was performed for 1 hr at 4 °C with 1/5 volume precipitation buffer. The phage particles were pelleted for 30 min at 20,000× g and 4 °C (Sorvall Centrifuge RC5B Plus, Rotor SS34) and resuspended in 1 mL 1X PBS. Remaining bacteria were pelleted for 2 min at 16100× g (Eppendorf Centrifuge 5415 D) and supernatants containing the oligopeptide phage libraries were collected and stored at 4 °C.

Phage Library Biopanning

To reduce background signals, serum used for biopanning was precleared from antibodies reactive with phage particles. Therefore, two wells of a 96-well ELISA plate (Costar) were coated with 4 × 10^{10} c.f.u, Hyperphage in 300 μL phosphate buffer saline (PBS). The protein binding capacity of the well surface was saturated with 300 μL blocking solution (PBS supplemented with 2% skim milk powder (BD) and 0.1% Tween 20) per well. The blocking solution was removed and the mouse sera from germ-free mice (GF) and SFB-monocolonized mice (SFB mono) (1:200 dilution in 300 μL blocking buffer) were incubated for 1 hr in each of the two wells (total 2 hr) with immobilized "Hyperphage" to preclear anti-phage serum antibodies.

For antibody-based phage display, precleared serum from germ free and SFB monocolonized mice, or luminal contents from Taconic B6 mice was transferred into 2 wells (150 μL each) previously coated with anti-mouse IgA or IgG antibodies and saturated with blocking buffer to capture antibodies used for the panning procedure. Excess antibodies and other non-specific proteins were removed by washing 3 times with washing buffer (PBS supplemented with 0.05% Tween 20). For the selection of oligopeptides specific to germ-free serum antibodies, the phage library was incubated with immobilized GF serum antibodies for 1 hr at room temperature and then unbound phage were removed and placed onto wells containing serum from SFB monocolonized mice and further incubated for 2 hr at room temperature.

Unbound oligopeptide phage was removed by stringent washing (10 times with washing buffer). Bound oligopeptide phage particles were eluted with 200 μL elution buffer (10 μg/mL trypsin in PBS) per well for 30 min at 37 °C. The eluted phage titer was

determined using 10-fold dilutions of 10 μL of the elution followed by *E. coli* TG1 infection and plating onto 2× YT agar supplemented with ampicillin. To amplify the eluted phage for input in the next panning round, the remaining 190 μL of elution were used to infect 1 mL of an *E. coli* TG1 culture (OD_{600} = 0.5) for 30 min at 37 °C. Cells were plated on 10 cm 2× YT-GA agar plates and incubated at 37 °C overnight to allow amplification of eluted phage for the next panning round. The cells were scraped using 5 mL of 2× YT-GA. To produce phage, 30 mL of 2× YT-GA were inoculated (OD_{600} < 0.1) with the scraped cells and grown up to OD_{600} = 0.5. Phage particles were produced following the same procedure as described above for packaging of oligopeptide phage libraries. Amplified phage was precipitated only once (1 hr on ice) after adding 1/5 volume precipitation buffer. After pelleting (1 hr at 4 °C, 3,220× g), the phage was resuspended in 1000 μL of 1X PBS. Remaining bacteria were pelleted for 10 min at 15000× g, the amplified oligopeptide phage containing supernatant was collected and stored at 4 °C until used as input phage for the next panning round. After the fourth panning round for serum antibodies, or third round for gut antibodies, 10-fold dilutions of eluted phage were used to infect 50 μL *E. coli TG1* (OD_{600} = 0.5), the cells were plated on 2× YT-GA agar plates and incubated at 37 °C overnight to obtain single colonies that allow screening of monoclonal oligopeptide phage. To screen the enriched clones after the third round of each panning for immunogenic oligopeptides, 96 randomly selected clones were analyzed by monoclonal phage ELISA.

Monoclonal Phage ELISA

To screen clones obtained from biopanning monoclonal phage were produced. A 96-well microtiter plate was supplemented with 180 μL 2× YT-GA medium, inoculated with single colonies after the fourth panning round and incubated (37 °C, 300 rpm) overnight. For phage production, 175 μl 2× YT-GA per well were inoculated with 10 μL of the overnight culture and incubated for 2 hr at 37 °C and 300 rpm to reach logarithmic growth. Cells were infected with 5 × 10^9 cfu Hyperphage (M13K07ΔgIII) for 30 min at 37 °C. To ensure antibiotic resistance, cells were incubated for 30 min at 37 °C and 300 rpm. To change the medium for phage production, the cells were pelleted for 10 min at 3,220× g and resuspended in 180 μL 2× YT-AK followed by phage production at 30 °C and 300 rpm overnight. Cells were pelleted and supernatant containing phage used for monoclonal phage ELISA.

To capture phage, rabbit anti-M13 (pVIII specific, 1:5,000 in PBS, PA1- 26758 Thermo Scientific) was immobilized on an ELISA plate (Costar) at 4 °C overnight. Wells were saturated with blocking buffer for 1 hr at room temperature. Plates were washed 3 times with washing buffer before addition of monoclonal phage (50 μL in 100 μL blocking buffer). Phage particles were captured for 2 hr at room temperature. To reduce background phage binding, mouse serum samples (1:500) were precleared in blocking buffer containing 10^{10} cfu/mL Hyperphage for 2 hr at room temperature. Remaining monoclonal phage were removed by 3 washing steps with washing buffer and the precleared sera or luminal antibodies were transferred to the wells containing immobilized oligopeptide phage particles and incubated for 2 hr at room temperature. Serum or gut antibodies were removed by 3 washing steps and bound antibodies were detected using goat anti-mouse IgA and IgG antibodies conjugated with horseradish peroxidase (HRP) for 1 hr at room temperature. Excess detection antibody was removed by 3 washing steps and the ELISA developed with TMB substrate solution. Signals were detected using an ELISA reader at 450 nm using SpectraMax M2.

Isolation of luminal antibodies

Luminal antibodies were isolated by lavage of the entire small intestinal contents with 7ml sterile PBS supplemented with protease inhibitors (Thermo Scientific). Luminal contents were cleared by centrifugation and supernatant used for phage biopanning or ELISA.

Enzyme-linked immunosorbent assay (ELISA)

High binding ELISA plates (Corning) were coated overnight at 4 °C with 2.5 μg/ml of SFB3340 protein. Plates were blocked with 2% skim milk in PBS prior to sample incubation. For serum and luminal samples, plates were incubated with serially diluted serum or luminal samples. For cloned mAbs, plates were incubated with serially diluted mAbs starting at 10 ng/ml. Positive controls for reactivity to Ovalbumin (clone F2-3.58, BioXCell), Bovine Serum Albumin (Polyclonal, SouthernBiotech), dsDNA (sera from NZB/W mice) and LPS (clone SLP-32, Sigma-Aldrich) were used. Each sample was plated in duplicate. Bound antibodies were detected using peroxidase conjugated goat antibodies to IgA (SouthernBiotech), IgG1 (SouthernBiotech), IgG2b (SouthernBiotech), IgG2c (Jackson Lab), IgM (Jackson Immunoresearch) at 1:5000 dilution in PBS. For mAbs, bound antibodies were detected with mouse anti-human IgG-HRP. Absorbance was measured at 450 nm using SpectraMax M2.

ELISpot

Multiscreen 96-well ELISPOT plates (Millipore) were coated overnight at 4 °C with 2.5 ug/ml of SFB3340 protein. Plates were blocked with 10% FBS in complete RPMI (GIBCO). Cells from various tissues were serially diluted in complete RPMI and plated onto coated ELISPOT plates and incubated at 37°C overnight. Cells were washed off and following washes with PBS, secondary peroxidase conjugated goat antibodies to IgG1, IgG2b and IgA (Southern Biotech) were used at 1:1000 in PBS to detect antibody-secreting cells. Plates were developed with AEC developing reagent (Vector Laboratories) according to manufacturer's instructions. Plates were read on an ImmunoSpot C.T.L. Analyzer and quantitated using ImmunoSpot.

Tetramer generation

Recombinant SFB3340 protein was procured from GenScript, biotinylated at 1:1 ratio using EZ-Link™ Sulfo-NHS-LC-Biotin (ThermoFisher) and tetramerized with streptavidin-PE (Prozyme) as previously described.[43] Decoy reagent to gate out non-$SFB3340^+$ cells was made by conjugating SA-PE to DyLight™ 594 NHS Ester (ThermoFisher), washing and removing any unbound

DyLight™ 594, and incubating with an excess of an irrelevant biotinylated decoy peptide bearing the affinity purification tags present in SFB3340 protein used for tetramer generation, specifically, a 31 mer peptide (HHHHHHENLYFQGGSGGLNDIFEAQKIEWHE) containing His tag, TEV cleavage sites and AviTag sequence was used to make the decoy reagent. As such, despite inclusion of His tag, TEV cleavage and AviTag sequences in the recombinant SFB3340 protein, these domains were not removed prior to tetramer generation.

De novo colonization with SFB containing feces

For SFB colonization, fresh fecal pellets collected from *Rag2*$^{-/-}$*Il2rg*$^{-/-}$ mice were resuspended in PBS and clarified by centrifuging the bacterial pellet at 300g, prior to oral gavage.

Quantification of fecal DNA

Fecal DNA was prepared using the Quick-DNA Fecal/Soil Microbe DNA Miniprep Kit (Zymo Research) according to the supplier's protocol. For generating a standard curve of qPCR, SFB 16S rRNA gene fragment was cloned into the pCR™2.1-TOPO™ vector (ThermoFisher) using TA cloning. A serial 10-fold dilution of 10^2, 10^3, 10^4, 10^5, 10^6,10^7,10^8 and 10^9 copies of the recombinant plasmid DNA containing the SFB 16S rRNA gene fragment was used. Two pairs of SFB 16S rRNA gene-based qPCR primers, SFB736F (5′-GACGCTGAGGCATGAGAGCAT-3′)/SFB844R (5′- GACGGCACGGATTGTTATTCA-3′) were used in a 7500 Fast Real-Time PCR System (Life Technologies) to quantify SFB colonization in the feces. Briefly, a 10μl mixture containing 50ng of template, 1μl of the primer mixture containing 100 nM of each of the forward and reverse primers, 5μl of 2 x SYGR green Fast master mix (Life Technologies) were used to set up the reaction.

Flow cytometry

Single-cell suspensions were prepared and resuspended in 50μl in PBS containing Fc block (2.4G2) and first incubated with decoy tetramer at a concentration of 10 nM at room temperature for 10 min. SFB3340-PE tetramer was added at a concentration of 10 nM and incubated on ice for 30 min along with surface antibodies followed by intracellular antibody staining when needed. All cells were run on a BD Symphony A5 cytometer and analyzed using FlowJo software.

Isolation of leukocytes from tissues

Cells from Peyer's patches, mesenteric lymph nodes, spleen and bone marrow were collected in complete media (RPMI, 3% heat inactivated FCS, 10 mM HEPES, 1% Pen/Strep). The tissue was mashed through a 70μm cell strainer to generate single cell suspensions. For lamina propria, the small intestine was dissected and opened longitudinally and cut into 4-cm pieces, followed by incubation in RPMI, 3% heat inactivated FCS, 5 mM EDTA (Sigma-Aldrich), 0.145 mg/ml DTT (Sigma-Aldrich) at 37°C for 20 minutes on a stirring platform. To separate the intestinal epithelial lymphocyte (IEL) and lamina propria (LP) layer, intestinal contents were transferred through a sterile fine-meshed kitchen strainer into a 500 ml beaker. Strainer was tapped on beaker several times after straining and pieces of small intestine were transferred to a 50 ml conical tube containing 10 ml of serum free media with 2mM EDTA per intestine. After shaking the tube vigorously for 30 seconds, the contents of the tube were strained through the strainer into the beaker. The process was repeated three times. The tissue was minced finely in the digest containing RPMI with 0.1 mg/ml Liberase TL (Roche) and 1mg/ml DNase I (Sigma-Aldrich), with continuous stirring at 37°C for 25 min. Digested tissue was passed through 100 μm cell strainers. Lymphocytes were further enriched by centrifugation at room temperature at 695 g for 8 min in 37.5% Percoll (GE Healthcare), prior to washing and resuspension for downstream analysis.

Single-cell RNA-sequencing

Peyer's patch leukocytes from 10 WT B6 mice de novo colonized for 21 days with SFB were separately stained with oligo hashtagged antibodies (TotalSeqC 1 – 10, Biolegend), prior to pooling, staining, and FACS isolation of SFB3340$^+$ B cells. A single cell suspension was prepared from pooled sorted cells and loaded onto one channel on the 10x Chromium Controller (10x Genomics) according to the manufacturer's protocol, with a target capture of 10,000 cells per channel. Sequencing libraries were generated using the NextGEM Single Cell 5' Kit v2. Gene expression, BCR, and feature barcoding libraries were pooled and treated with Illumina Free Adapter Blocking Reagent (Illumina). Sequencing of pooled libraries was carried out on a NextSeq 2000 sequencer (Illumina), using a NextSeq P2 flowcell (Illumina), with target depths of 40000, 5000, and 5000 raw reads per cell for gene expression, BCR, and feature barcode libraries, respectively. Basecalls were converted to FASTQs and processed to gene counts, hashtag counts, and assembled BCR sequences using Cell Ranger v. 6.1.1, with the GRCm38 genome annotation and V(D)J reference, using default parameters and cell calling with an expected cell number of 10000.

Single-cell RNA-sequencing quality control and demultiplexing

Filtering, normalization, projection, and clustering of 10x data was conducted using Seurat Toolkit v.4.4.3.[58] Cell Ranger processing yielded 2984 10x barcodes called as putative cells. To limit analysis to high-quality single cells, quality filters were applied to the gene count data using the following empirical thresholds: total genes detected $\geq$ 250 and $\leq$ 6000, UMI counts $\geq$ 1400 and $\leq$ 35000, mitochondrial UMIs $\leq$ 20%, ribosomal protein UMIs $\leq$ 50%, and hemoglobin UMIs $\leq$ 10%. To limit analysis to B cells, we excluded barcodes expressing genes characteristic of other cell types (raw UMI counts: Cd3d $\geq$ 3, Cd3e $\geq$ 3, Vil1 $\geq$ 1, Reg3g $\geq$ 2), and retained only barcodes expressing characteristic B cell genes (log-normalized UMI counts: Cd74 $\geq$ 2, H2-Ab1 $\geq$ 0.5,

Cd79a ≥ 0.5, Ly6e ≥ 0.5, Cd52 ≥ 0.25). We used empirical thresholds on the log-counts-per-million hashtag UMIs to call each barcode as positive or negative for each hashtag, and kept cells that were positive for a single hashtag. After quality filtering and demultiplexing, we retained 1762 high-quality single B cells for downstream analysis.

Gene expression data were log-normalized, projected onto a UMAP embedding, and clustered using shared nearest neighbor modularity optimization as implemented in Seurat. Cluster identity was determined using marker gene expression and confirmed using Ig isotypes based on heavy chain alignments in the assembled BCR sequences.

Analysis of BCR sequence data

We analyzed BCR sequence data using the Immcantation toolkit (https://immcantation.readthedocs.io/en/stable/). Starting from the assembled BCR contig FASTA files output by cellranger, Ig regions and gene usage for each sequence were determined using Change-O.[59] BCR clones were identified independently for heavy and light chains using Change-O, using optimal clone distances estimated with Shazam.[59] Heavy chain clones were filtered to include only those with consistent light chain sequences, and germline sequences were inferred at the nucleotide level. BCR lineages were estimated from the full amino acid sequences using the parsimony ratchet,[60] as implemented in the R package phangorn.[61]

Recombinant antibody production

Recombinant antibodies derived from recurrent public clonotypes were generated by WuXi Biologics in a human IgG1 backbone.

Site directed mutagenesis (SDM)

SDM was carried out using germline sequences from two public (V_H1-76(RC) and V_H1-53(RC)) clonotypes as DNA template. Mutagenic primers were designed using PrimerX. Briefly, 50 ng of template DNA, 0.5 μM forward and reverse primer, Phusion High–Fidelity DNA Polymerase (Thermo Scientific) were used, and annealing temperature was set to 58°C. After PCR, the reaction was treated with 1μl of DpnI (New England Biolabs) to degrade parental DNA. The digested DNA sample was purified using a spin column (Zymo Research) and transformed into chemically competent Stbl3 cells. The colonies obtained were verified using Sanger sequencing.

Recombinant antibody production for SDM

Expi293F cells were cultured in Expi293 Expression Medium following manufacturer's instructions. (Thermo Scientific). Cells were transfected with 625 ng of IgH and corresponding IgL chain vector DNA in 24-well deep-well plates using the Expi293 Transfection Kit. Cells were grown at 37°C, 8% CO2, and 250 rpm for 6 days. On day 6 post transfection, the culture supernatant was harvested and loaded on a protein G column. The column was washed with PBS, and the IgG protein was eluted with a low pH buffer followed by buffer exchange in 1X PBS.

Biolayer Interferometry

All assays were performed on the Octet Red Instrument (ForteBio) at 30C with shaking at 1,000 RPM. Purified antibodies were captured using Anti-Human IgG Fc capture (AHC) biosensors by immersing sensors into KB buffer (1X PBS, 0.01% BSA, 0.02% Tween 20, and 0.005% NaN_3) containing individual antibodies at a standard concentration of 10μg/mL for 300s. After loading, baseline signals were recorded for 60s in KB. The sensors were then immersed in wells containing SFB3340 at a standard concentration of 250nM in KB for 300s (association phase). Following this, sensors were immersed in KB for an additional 300s (dissociation phase). Rmax values were recorded as the max nm shift at the end of the association phase. All binding experiments were run twice for each antibody, and mean Rmax values were reported.

Immunofluorescence staining

Ileal tissue from R2G2 mice was flushed with cold PBS, splayed open and rolled into a Swiss roll, then fixed in 4% paraformaldehyde (PFA) for 4hr and placed in 30% sucrose overnight at 4°C. Next day rolls were shaken gently in OCT for 2hr and then embedded in OCT.16 μm sections were cut on a cryotome, dried and then frozen at -80°C. Tissues were blocked and permeabilized using 5% Rat IgG, 5% BSA, 0.3% Triton-X in PBS for 1 hr. Tissues were stained with Alexa Fluor® 488 anti-mouse EpCAM (1:200 dilution in 5% BSA in PBS) antibody and recombinant mAb V_H1-76RC N1 overnight at 4°C. Anti-human IgG1-R718 (1:100 dilution in 5% BSA in PBS) was used as a secondary antibody. Images were acquired using an SP5 confocal microscope (Leica).

QUANTIFICATION AND STATISTICAL ANALYSIS

Statistical analysis was performed in Prism (GraphPad Software, v10). Unpaired, two-tailed Student's t tests were applied to determine the differences between two individual groups. For statistical details of specific experiments, please see respective figure legends.